Intrinsic chiral magnetic effect in Dirac semimetals due to dislocations

Maxim N. Chernodub, Mikhail Zubkov

Intrinsic chiral magnetic effect in Dirac semimetals due to dislocations

M. N. Chernodub[1, 2, *] and Mikhail Zubkov[3, 4, 2, 1, †]

[1] *CNRS, Laboratoire de Mathématiques et Physique Théorique, Université François-Rabelais, Fédération Denis Poisson - CNRS, Parc de Grandmont, Université de Tours, 37200 France*

[2] *Far Eastern Federal University, School of Biomedicine, 690950 Vladivostok, Russia*

[3] *Institute for Theoretical and Experimental Physics, B. Cheremushkinskaya 25, Moscow, 117259, Russia;*

[4] *Moscow Institute of Physics and Technology, 9, Institutskii per., Dolgoprudny, Moscow Region, 141700, Russia*

(Dated: August 1, 2015)

A dislocation in a Dirac semimetal carries an emergent magnetic flux parallel to the dislocation axis. We show that due to the emergent magnetic field the dislocation accommodates a single fermion massless mode of a corresponding low-energy one-particle Hamiltonian. The mode is propagating along the dislocation with its spin directed parallel to the dislocation axis. In agreement with the chiral anomaly observed in Dirac semimetals, an external electric field to the spectral flow of the one-particle Hamiltonian by pumping the fermionic quasiparticles out from vacuum and creating a nonzero axial (chiral) charge in the vicinity of the dislocation. In the presence of the chirality imbalance, the intrinsic magnetic field of the dislocation generates an electric current along the dislocation axis. We point out that this effect – which is an "intrinsic" analogue of the chiral magnetic effect – may experimentally reveal itself through transport measurements in Dirac semimetals via enhanced conductivity when the external electric field is parallel to the dislocation axis.

I. INTRODUCTION AND MOTIVATION

The Dirac semimetals are novel materials that have been discovered recently (Na_3Bi and Cd_3As_2 [1–3]). A possible appearance of Dirac semimetals in the other systems (for example, $ZrTe_5$ [4], and Bi_2Se_3 [5]) was also discussed. In Dirac semimetals the fermionic quasiparticles propagate according to the low energy action that has emergent relativistic symmetry. Both in Na_3Bi and Cd_3As_2 there exist two Fermi points $\pm\boldsymbol{K}^{(0)}$. At each Fermi point the pair of left-handed and right-handed fermions appears. The Dirac semimetals represent an arena for the observation of various effects specific for the high energy physics. In particular, the effects of chiral anomaly play an important role in physics of these materials [3, 6–10].

In the Weyl semimetals, which were also discovered recently (in particular, TaAs [11]) one of the two Fermi points hosts a right-handed Weyl fermion while another Fermi point hosts a left-handed Weyl fermion. Various relativistic effects were discussed in Weyl and Dirac semimetals already before their experimental discovery [12–24].

In [4] the experimental observation of chiral anomaly and chiral magnetic effect in $ZrTe_5$ was reported as measured through their contributions to the conductance of the sample. It has been shown, that in the presence of parallel external magnetic field and external electric field the chiral anomaly leads to the appearance of nonzero chiral density and nonzero chiral chemical potential. The latter drives ordinary chiral magnetic effect [25], which generates dissipationless electric current directed along the magnetic field. This work was followed be a number of papers, where the experimental detection of chiral anomaly was reported in different Dirac and Weyl semimetals (see [26] and references therein).

Similar to graphene [27–34] in the presence of elastic deformations the fermionic quasiparticles in Dirac and Weyl semimetals experience emergent gauge field and emergent gravity (see, for example, [35–38] and references therein). In this paper we will concentrate on dislocations in the crystalline order of the atomic lattice, which are particularly interesting cases of the elastic deformations of the ion crystal lattice [39]. The dislocation is a line-like defect characterized by the Burgers vector $\boldsymbol{b}$ which determines the physical displacement of the atomic lattices along the dislocation. The vector $\boldsymbol{b}$ is a global characteristic of the dislocation because it is a constant quantity over the entire length of the dislocation. In rough terms, one may imagine the dislocation as a vortex which possesses a fixed "vorticity" given by the Burgers vector $\boldsymbol{b}$. The extreme examples of the dislocations are the screw dislocation (shown in Fig. 1) and the edge dislocation (illustrated in Fig. 2) for which the corresponding Burgers vectors are parallel and, respectively, perpendicular to dislocations' axes $\boldsymbol{n}$. There are other types of the dislocations lying in between these two extreme cases.

In [38] the effect of the dislocation on the geometry experienced by fermionic quasiparticles in Dirac semimetals was considered for the first time. Aharonov-Bohm effect and Stodolsky effect (the latter effect describes a correction to the Aharonov-Bohm effect due to torsion) were investigated for the scattering of the quasiparticles on dis-

* maxim.chernodub@lmpt.univ-tours.fr; on leave from ITEP, Moscow, Russia.

† zubkov@itep.ru

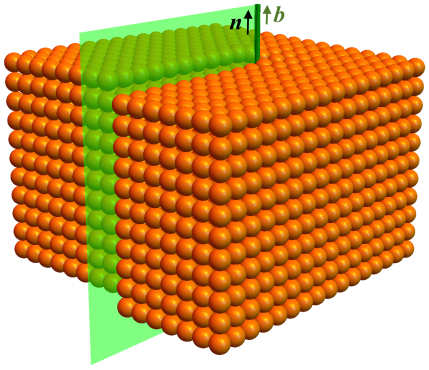

FIG. 1. Illustration of the screw dislocation of the atomic lattice with the Burgers vector $\boldsymbol{b}$ parallel to the axis $\boldsymbol{n}$ of the dislocation (the green line). The semitransparent plane points out to the region where the atomic planes experience a shift.

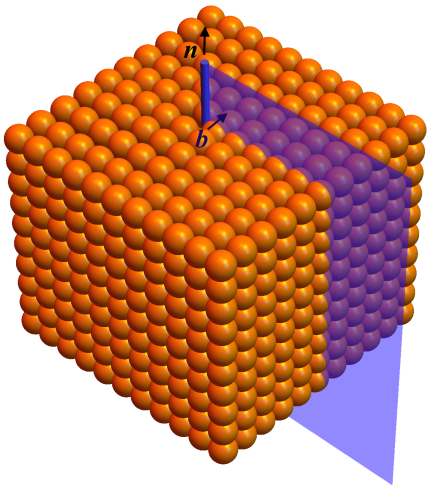

FIG. 2. Illustration of the edge dislocation with the Burgers vector $\boldsymbol{b}$ perpendicular to the dislocation axis $\boldsymbol{n}$ (the blue line). The semitransparent plane shows the extra half-plane of ions introduced in the crystal.

locations. Besides, basing on an obvious analogy with the results of [4] it was proposed, that the dislocation (that carries an emergent magnetic flux) becomes the source of chiral anomaly and chiral magnetic effect. This occurs because the dislocation carries emergent magnetic field. Therefore, it was argued, that the chiral anomaly and chiral magnetic effect occur without any external magnetic field. According to [38] the contribution of topology to magnetic flux Φ is equal to the scalar product $\boldsymbol{K}^{(0)}\boldsymbol{b}$, where $\boldsymbol{b}$ is the Burgers vector. There may also appear the contribution to the flux Φ proportional to the tensor of elastic deformations caused by the dislocation with the coefficients of proportionality that are analogous to the Gruneisen parameter of graphene. The emergent magnetic flux is associated with emergent magnetic field The emergent magnetic flux is associated with emergent magnetic field

$$H^i(x) = \Phi \int dy^i \delta^{(3)}(x-y), \tag{1}$$

where the integral is taken along the dislocation. The appearance of the delta-function in Eq. (1) in the low-temperature theory corresponds to the fact that the emergent magnetic flux localized within the dislocation core of the radius $\xi \sim a$ which is of the order of the interatomic distance a.

Next, in [38] the simple model of the dislocation was used, in which it is represented as a tube of size ξ with the emergent magnetic field inside it. In the presence of external electric field directed along the dislocation the naive expression for the chiral anomaly reads as follows[1]:

$$\langle \partial_\mu j^\mu_5 \rangle = \frac{1}{2\pi^2} \boldsymbol{E}\boldsymbol{H}\,, \tag{2}$$

where $j^\mu_5 = j^\mu_R - j^\mu_L$ is the chiral current given by the difference of the currents of the right-handed and left-handed quasiparticles.

The corresponding naive expression for the chiral magnetic effect [25] has the form

$$\boldsymbol{j} = \frac{\mu_5}{2\pi^2}\boldsymbol{H}\,, \tag{3}$$

where $j^\mu = j^\mu_R + j^\mu_L$ is the electric current given by the sum of the currents of the right-handed and left-handed quasiparticles. The chiral chemical potential μ_5 is the difference between the chemical potentials associated with the fermions of right-handed and left-handed chiralities:

$$\mu_5 = \frac{1}{2}\left(\mu_R - \mu_L\right)\,. \tag{4}$$

The chiral magnetic effects generates a dissipationless electric current $\boldsymbol{j}$ the direction of magnetic field $\boldsymbol{H}$ in the presence of the chiral imbalance encoded into the chiral chemical potential μ_5.

The further examination of the mentioned above problem has led us to the conclusion, that the naive application of the pattern of chiral anomaly discussed in [4] to the case, when the magnetic field is emergent and is caused by dislocations, has certain restrictions. Strictly speaking, the mentioned above model of the fermionic excitations and chiral anomaly within the dislocation may be applied to the investigation of real materials only if the emergent magnetic flux of the low energy field theory is distributed within the area of size ξ essentially larger, than the interatomic distance a while the emergent magnetic flux of the dislocation is essentially larger, than 2π. In this situation we are formally able to use the

[1] Hereafter we adopt the relativistic system of units $c = \hbar = 1$, so that all dimensional quantities are expressed in units of eV. For simplicity, we also absorb the elementary charge e into the definition of electromagnetic field.

low energy field theory for the description of fermionic excitations inside the dislocation core, and apply Eqs. (2) and (3). This opportunity requires an additional investigation, which is out of the scope of the present paper. Presumably, it may occur only for the strong dislocations with sufficiently large values of Burgers vector $\boldsymbol{b}$, when the crystal lattice is distorted considerably (or for the case, when many parallel dislocations with small values of the Burgers vectors are located close to each other).

In the present paper we consider the opposite situation, when in Dirac semimetals the values of Burgers vector are relatively small, so that the magnetic flux at the dislocation is smaller than 2π or around 2π. In this situation the crystal structure is not violated strongly, so that the dislocation core size is, presumably, of the order of the interatomic distance $\xi \sim a$. The low energy theory is developed for the states with the typical values of momenta much smaller, that $1/a$. Therefore, in this case the states localized within the dislocation core cannot be described by the field theory. In order to describe such states the microscopic theory is to be applied.

It appears, that in the microscopic case the expressions for the anomaly in the quasiparticle currents and for the chiral magnetic effect caused by the emergent magnetic field of the dislocation, differ from the mentioned above naive expressions (2) and (3), respectively. In particular, the anomaly in the right- and left-handed quasiparticle currents is given by

$$\langle \partial_\mu j^\mu_{R,L} \rangle = \pm \frac{1}{4\pi^2} \boldsymbol{E}\boldsymbol{B} \quad \text{or} \quad \langle \partial_\mu j^\mu_5 \rangle = \frac{1}{2\pi^2} \boldsymbol{E}\boldsymbol{B}\,, \qquad (5)$$

where the upper and lower signs in the first equation correspond to the right-handed and left-handed quasiparticles, respectively. The formula for the chiral magnetic effect

$$\boldsymbol{j}^{\rm CME} = \frac{1}{2\pi^2}\mu_5 \boldsymbol{B}\,, \qquad (6)$$

is also modified compared to Eq. (3). The important difference between Eqs. (2), (3) and (5), (6) is that the effective magnetic field $\boldsymbol{B}$ – contributing to the anomaly (5) and to the chiral magnetic effect (6) – differs from the emergent magnetic field at the dislocation $\boldsymbol{H}$ as given in Eq. (1).

The basic reason for the difference between the emergent magnetic field $\boldsymbol{H}$ and the effective magnetic field $\boldsymbol{B}$ is that the emergent magnetic field $\boldsymbol{H}$ of the dislocation has a very low (of the order of unity or even smaller) magnetic flux Φ. In this case the contribution to both mentioned effects is given by a single fermionic mode (we call it "zero mode") propagating along the dislocation rather then by a large ensemble of the lowest Landau modes with a huge degeneracy factor. To be more precise, the effective magnetic field $\boldsymbol{B}$ is expressed through the probability density corresponding to the zero mode of the one-particle Hamiltonian in the background of the emergent magnetic field $\boldsymbol{H}$ due to the dislocation. The appearance of the propagating (zero) mode at the dislocation is a natural effect, which is known to exist in topological insulators with lattice dislocations [44].

The contribution of the individual zero mode to both chiral anomaly (5) and the chiral magnetic effect (6) can be described with the help of the effective magnetic field $\boldsymbol{B}$, which carries exactly a unit of the elementary magnetic flux contrary to the original emergent magnetic field $\boldsymbol{H}$ which may have an arbitrary (but still small) value of the total flux Φ, in general. The effective field $\boldsymbol{B}$ is localized in the wide area of linear size ξ_0, where $1/\xi_0$ is the infrared cutoff of the considered field theoretical low energy approximation (below we argue that ξ_0 may be identified with the mean free path of the quasiparticles which is, for example, $\xi_0 \sim\sim 200\,\mu$m for Cd_3As_2 [7]).

In this paper we demonstrate that for a straight screw dislocation directed, for example, along the symmetry axis of the crystal the emergent magnetic flux associated with the emergent field $\boldsymbol{H}$ is given by

$$\Phi = \left(\boldsymbol{K}^{(0)} \cdot \boldsymbol{b}\right) + \frac{\beta}{2a}(\boldsymbol{n}\cdot\boldsymbol{b})\,, \qquad (7)$$

where the first term is of the topological origin [38] while the second term is not topological (here β is an analogue of the Gruneisen parameter of graphene [32]). The magnetic field associated with the flux (7) is localized within the dislocation core of a typical size $\xi \sim a$, where $a \sim 1\,n$m is a typical interatomic distance. In Eq. (7) the vector $\boldsymbol{K}^{(0)}$ encodes positions of the Fermi points $\boldsymbol{k} = \pm\boldsymbol{K}^{(0)}$ in the momentum space and $\boldsymbol{n}$ is the direction of the dislocation axis. For a straight screw dislocation the vectors $\boldsymbol{K}^{(0)}$, $\boldsymbol{b}$ and $\boldsymbol{n}$ in Eq. (7) are parallel to each other.

We will discuss effects which appear due to the interplay between quantum anomaly and dislocations in the crystal structure of Dirac semimetals. A fermion excitation is affected by the dislocation, in particular, via the mentioned above intrinsic magnetic field which is localised in a spacial vicinity of the dislocation and directed along the axis of the dislocation. In principle, the emergent magnetic fields corresponding to different Weyl fermions (that belong to different Fermi points and/or have different chiralities) differ from each other. However, there exists an approximation, in which those emergent fields $\boldsymbol{H}$ have the same absolute values, but opposite directions for the two Fermi points $\pm\boldsymbol{K}^{(0)}$. If this approximation is not violated strongly (which is the general case) the signs of the emergent magnetic fluxes experienced by the quasiparticles living near to the Fermi points $\pm\boldsymbol{K}^{(0)}$ are opposite. In the Dirac semimetal both right- and left-handed fermion excitations are present in each (of the two) Dirac cone, therefore in this case we have a standard effective magnetic field $\boldsymbol{B}(\boldsymbol{x})$ acting on the right- and left-handed fermions at one Dirac cone and the magnetic field $-\boldsymbol{B}(\boldsymbol{x})$ acting on the right- and left-handed fermions at another cone. These fields enter expression for the anomaly Eq. (5).

If now one applies an external static electric field $\boldsymbol{E}$ along the axis of the dislocation, then the quantum

anomaly will generate the chiral charge at a rate proportional to the scalar product $\boldsymbol{EB}$. The generated chiral charge will dissipate, both due to chiral-changing processes inside the core of the dislocation and due to a spatial diffusion of the chiral charge around the core. Next we notice that the equilibrium distribution of the chiral charge – which can effectively be described by a spatially nonconstant but otherwise static chiral chemical potential μ_5 – is subjected to the intrinsic magnetic field of the dislocation itself. The chemical potential μ_5 is distributed around the dislocation with the characteristic length L_V (for example, in Cd_3As_2 this length is of the order of $L_V \sim 2\,\mu$m.) The chirally imbalanced matter in the presence of magnetic field generates dissipationless electric current directed along the dislocation and concentrated in the spatial vicinity around it. Therefore, the intrinsic magnetic field of the dislocation would lead to a spatially-dependent (negative) magnetoresistance around the dislocation. Similar arguments were used in Ref. [4] to experimentally investigate the chiral magnetic effect in $ZrTe_5$ in the presence of external magnetic field.

The paper is organized as follows. In Sect. II we recall briefly general theory of quasi-relativistic fermions in Dirac semimetals in the presence of elastic deformations which lead to both emergent gauge field and emergent gravity (the latter is described by an emergent vielbein [40]). In Sections III and IV we discuss these effects focusing on dislocations, partially following Ref. [38]. In Sect. V we consider zero modes of the one-particle Hamiltonian and demonstrate, that there always exists a single mode with definite spin directed along the emergent magnetic flux, which is localized in a wide area around the dislocation. In Sect. VI we show that the spectral flow along the branch of spectrum (that crosses zero at the mentioned zero mode) gives rise to the anomalies in quasiparticle currents: in a Dirac semimetal the chiral anomaly appears. For the sake of simplicity, these results are discussed first for a strait dislocation which is directed along the symmetry axis z of the crystal which coincides with the direction of the Fermi point $\boldsymbol{K}^{(0)}$ in the momentum space. We extend our results to the case of strait dislocations with arbitrary direction in Sect. VII. Then in Sect. VIII we discuss the generation of the chiral charge via the chiral anomaly (5) due to interplay between an external electric field and internal magnetic field of the dislocation. We show in Sect. IX that the chiral background at the dislocation leads to a contribution to the electric conductivity of a Dirac semimetal via the chiral magnetic effect (6). In Sect. X we estimate the numerical value of the contribution to the conductance of Dirac semimetals in the presence of a dislocation. The last section is devoted to discussion and our conclusions.

II. RELATIVISTIC FERMIONS IN DIRAC SEMIMETAL

The Dirac semimetal possesses two cones, each of which hosts one right-handed and one left-handed Weyl fermion. In the presence of elastic deformations caused by the dislocation the action for a right-handed and left-handed Weyl fermions near a given Fermi point are, respectively, as follows [38]:

$$S_R=\frac{1}{2}\int d^4x|\boldsymbol{e}|\left[\bar\Psi i e_b^\mu(x)\sigma^b\mathcal{D}_\mu\Psi-[\mathcal{D}_\mu\bar\Psi]ie_b^\mu(x)\sigma^b\Psi\right], \quad (8)$$

$$S_L=\frac{1}{2}\int d^4x|\boldsymbol{e}|\left[\bar\Psi i e_b^\mu(x)\bar\sigma^b\mathcal{D}_\mu\Psi-[\mathcal{D}_\mu\bar\Psi]ie_b^\mu(x)\bar\sigma^b\Psi\right], \quad (9)$$

where

$$i\mathcal{D}_\mu = i\nabla_\mu + A_\mu(x) \quad (10)$$

is the covariant derivative corresponding to the emergent $U(1)$ gauge field A_μ, $\sigma^0=\bar\sigma^0=1$, and $\bar\sigma^a=-\sigma^a$ with $a=1,2,3$ are the Pauli matrices. The currents of the right- and left-handed quasiparticles are, respectively, as follows:

$$J_R^\mu = \bar\Psi i e_b^\mu(x)\sigma^b\Psi\,, \quad (11)$$

$$J_L^\mu = \bar\Psi i e_b^\mu(x)\bar\sigma^b\Psi\,. \quad (12)$$

Throughout this paper the internal $SO(3,1)$ indices are denoted by Latin letters $a,b,c,...$ from the beginning of the alphabet while the space-time indices are denoted by Greek letters or by Latin letters $i,j,k,...$ from the middle of the alphabet.

The vierbein field $e_a^\mu = e_a^\mu(x)$ is a 4×4 matrix which carries all essential information about anisotropy and the elastic deformations (caused, for example, by a dislocation) of the ion lattice of the Dirac crystal. It is convenient to introduce the inverse of the inverse vierbein field, $e_\mu^a = e_\mu^a(x)$, defined, naturally, as follows:

$$e_a^\mu(x)e_\nu^a(x)=\delta_\nu^\mu\,. \quad (13)$$

In our paper we always assume that the deformations are small so that the determinant of the vierbein field

$$|\boldsymbol{e}|\equiv\det(\boldsymbol{e}_\mu^a)\,, \quad (14)$$

never vanishes.

In the absence of elastic deformations the fields entering the actions (8) and (9) are simplified. In this case the emergent gauge field A_μ is the same for both left- and right-handed fermions, it does not depend on coordinates, and its spatial components A_i are determined by the position of the unperturbed Dirac point $\boldsymbol{K}^{(0)}$ while the time component vanishes, $A_0=0$.

In the absence of elastic deformations the vierbein can be chosen in a diagonal form,

$$e_a^{(0),\mu}=\begin{pmatrix} v_F^{-1} & 0 & 0 & 0\\ 0 & \nu^{-1/3} & 0 & 0\\ 0 & 0 & \nu^{-1/3} & 0\\ 0 & 0 & 0 & \nu^{2/3}\end{pmatrix}, \quad (15)$$

where the parameter $\nu \neq 1$ reflects the fact that the experimentally studied Dirac semimetals are anisotropic materials [1–3]. It is also convenient to introduce the spatial component of the undeformed vierbein (15):

$$e_a^{(0),i} \equiv \hat{f}_a^i = \begin{pmatrix} \nu^{-1/3} & 0 & 0 \\ 0 & \nu^{-1/3} & 0 \\ 0 & 0 & \nu^{2/3} \end{pmatrix}, \qquad (16)$$

with $i, a = 1, 2, 3$. The quantity $v_F^i \equiv v_F \hat{f}_i^i$ with fixed $i = 1, 2, 3$ has a meaning of the anisotropic Fermi velocity in i-th direction. The determinant (14) in the undeformed case is $|\boldsymbol{e}^{(0)}| = v_F$.

The low-energy effective field theory (8), (9) has the natural ultraviolet cutoff $\Lambda_{UV} \sim |\boldsymbol{K}^{(0)}|$ associated with the positions of the Dirac cones in the momentum space. In order to determine a natural infrared cutoff we notice that in our field-theoretical approximation the massless quasiparticles do not interact with each other since the effective actions (8) and (9) contain only bilinear fermionic terms while the gauge field A_μ is a classical non-propagating field. Therefore, the natural infrared cutoff for our approach is $\Lambda_{IR} = 1/\xi_0$, where the length ξ_0 may be identified with the mean free path of the massless quasiparticles. Indeed at the distances of the order of the mean free path ξ_0 we cannot neglect interactions between the quasiparticles and their scattering off defects of the atomic lattice which, in general, cannot be captured by Eqs. (8) and (9).

As an example, we mention that for the Dirac material Cd_3As_2 the mean free path ξ_0 was estimated in Ref. [7] to be of the order of 200 μm. In the above formulation of the low-energy theory, the Dirac point corresponds to zero energy. In real situation the crystals of semimetal may have nonzero Fermi energy at the level crossing points. In particular, in [41] the values of Fermi energy of the order of 10 meV were reported for Na_3Bi. In the following applications we assume, that in the real systems the value of Fermi energy may be neglected, or that the sample is doped in such a way, that the doping-induced chemical potential shifts the level crossing to the vanishing energy.

In the upcoming sections for simplicity we restrict ourselves to the case, when the dislocation is an infinite straight line directed along the symmetry axis z of the crystal, which coincides with the direction of the Dirac point $\boldsymbol{K}^{(0)}$ in the momentum space. We will return to a more general case of an arbitrarily aligned straight dislocation in Sect. VII.

Now let us consider the case when the atomic lattice of a Dirac semimetal is elastically deformed. The deformation is described by the displacement vector u^i which gives the displacements of the ions with respect to their positions with respect to the unperturbed semimetal. In the approximation of isotropic elasticity for a straight dislocation directed around the $z \equiv x_3$ axis the displacement vector u^a is given by:

$$u^a = -\theta \frac{b^a}{2\pi} + u^a_{\rm cont}, \qquad (17)$$

where θ is the polar angle in the plane orthogonal to the dislocation and b^a is the Burgers vector. The first term in the right hand side of Eq. (17) is discontinuous vector function as it has a jump by b^a at $\theta = 0$. The second, continuous part of displacement is given by [43]

$$u^k_{\rm cont}(\boldsymbol{x}_\perp) = -\frac{b^l}{4\pi}\frac{1-2\sigma}{1-\sigma}\left[\epsilon^{3kl}\log\frac{|\boldsymbol{x}_\perp|e^\gamma}{2R} + \frac{\epsilon^{3il}\hat{x}^i_\perp \hat{x}^k_\perp}{1-2\sigma}\right] \qquad (18)$$

where $\boldsymbol{x}_\perp = (x_1, x_2)$ are the transverse coordinates in the laboratory reference frame, $\hat{x}^i_\perp$ are respective unit angles in the transverse plane and σ is the Poisson ratio which is defined as the negative ratio of transverse to axial strain of the atomic crystal. Throughout this paper we shall work in the laboratory reference frame in which the positions of ions are their real 3d coordinates.

Notice, that for the screw dislocation when the Burgers vector directed along the dislocation axis, $\boldsymbol{b} = (0, 0, b_z)$, the continuous part of the displacement vector vanishes, $u^k_{\rm cont} = 0$. It is worth mentioning, that while the values of $u^k_{\rm cont}$ may be large, its derivatives are small for sufficiently small b because after the differentiation the expression in Eq. (18) tends to zero at $|\boldsymbol{x}_\perp| \to \infty$.

In the presence of elastic deformations, in principle, the emergent vielbeins (as well as the emergent gauge fields) may differ for the left-handed and the right-handed fermions incident at the given Dirac point.

Let us introduce tensor of elastic deformations [39]

$$u^{ij} = \partial^i u^j + \partial^j u^i\,, \qquad (19)$$

where we have neglected a part quadratic in u^i by assuming that the deformations are small. In general, the emergent vielbein around the dislocation may be expressed up to the terms linear in displacement vector as follows (see Ref. [38] for the details of the derivation):

$$\begin{aligned} e^i_a &= \hat{f}^i_a(1 + \frac{1}{3}\gamma^k_{knj}u^{nj}) + \hat{f}^k_a \partial_k u^i - \hat{f}^n_a \gamma^i_{njk} u^{jk} \\ e^i_0 &= -\frac{1}{v_F}\gamma^i_{0jk}u^{jk}, \quad e^0_a = 0 \\ e^0_0 &= \frac{1}{v_F}(1 + \frac{1}{3}\gamma^k_{kij}u^{ij}) \\ |\boldsymbol{e}| &= v_F(1 - \partial_i u^i - \frac{1}{3}\gamma^k_{kij}u^{ij}) \\ & a, i, j, k, n = 1, 2, 3 \end{aligned} \qquad (20)$$

The emergent gauge field is given by

$$\begin{aligned} A_i &\approx -\nabla_i(\boldsymbol{u}\cdot\boldsymbol{K}^{(0)})) + \frac{1}{a}\beta_{ijk}u^{jk}, \\ A_0 &= \frac{1}{a}\beta_{0jk}u^{jk}, \quad i, j, k = 1, 2, 3 \end{aligned} \qquad (21)$$

The tensors β and γ, which are the analogues to the Gruneisen parameters in graphene, may, in principle be different for the right-handed and the left-handed fermions. The analogy to graphene prompts that their values could be of the order of unity. Notice, that in graphene the emergent electric potential A_0 does not arise outside of the dislocation core [32]. In the same

way we assume, that in the semimetal the parameters β_{0jk} may be neglected. The reason for this is that the combination $\boldsymbol{K}^{(0)}+\boldsymbol{A}$ appears as the value of momentum $\boldsymbol{P}$, at which the one-particle Hamiltonian $\mathcal{H}(\boldsymbol{x},\hat{\boldsymbol{P}})$ vanishes (one substitutes $\boldsymbol{K}^{(0)}+\boldsymbol{A}$ instead of the momentum operator $\hat{\boldsymbol{P}}$):

$$\mathcal{H}\big(\boldsymbol{x},\boldsymbol{K}^{(0)}+\boldsymbol{A}(\boldsymbol{x})\big)=0 \tag{22}$$

As a result we expand the Hamiltonian near the floating Fermi point $\boldsymbol{K}^{(0)}+\boldsymbol{A}(\boldsymbol{x})$:

$$\mathcal{H}(\boldsymbol{x},\hat{\boldsymbol{P}})=|\boldsymbol{e}(\boldsymbol{x})|\,e_a^k(\boldsymbol{x})\sigma^a\circ\Big[\hat{P}_k-\big(K_k^{(0)}+A_k(\boldsymbol{x})\big)\Big] +A_0(\boldsymbol{x})\,, \tag{23}$$

where by the symbol $\circ$ we denote the symmetric product

$$A\circ B=\frac{1}{2}(AB+BA). \tag{24}$$

The only possible source of $A_0(\boldsymbol{x})$ is the noncommutativity of momentum $\hat{\boldsymbol{P}}$ and coordinates. This means, that unlike A_k with $k=1,2,3$ the emergent electric potential A_0 is proportional to the derivatives of the parameters entering $\mathcal{H}(\boldsymbol{x},\hat{\boldsymbol{P}})$. The field A_k with $k=1,2,3$ is proportional to $1/a$ times the combination of the dimensionless parameters while A_0 is proportional to their derivatives but it does not contain the factor $1/a$. For slow varying elastic deformations this means that A_0 may be neglected. This consideration does not work, however, within the dislocation core, where physics is much more complicated. The influence of this unknown physics on the quasiparticles with small values of momenta (described by the action of the form of Eqs. (8), (9)) may be taken into account through the same emergent fields $A_\mu,\mu=0,1,2,3$ and e_a^k, which become strong within the dislocation core. The component of A_0 of emergent electromagnetic field is not forbidden by any symmetry. Therefore, it appears and gives rise to emergent electric potential (either attractive or repulsive) within the dislocation core.

Notice, that the simple model of Weyl semimetal with cubic symmetry has been considered in [35], where the following expression for the emergent gauge field was discussed ($i=1,2,3$):

$$A_i\approx-\nabla_i(\boldsymbol{u}\cdot\boldsymbol{K}^{(0)}))+\frac{1}{a}\Big(\beta u^{3i}+\beta'\delta_{i3}u^{33}\Big)\,, \qquad A_0=0\,. \tag{25}$$

A Dirac semimetal (with cubic symmetry) may, in principle, be described by the two copies of the model of [35].

III. EMERGENT MAGNETIC FLUX CARRIED BY THE DISLOCATION

In order to calculate the emergent magnetic field we should use integral equation

$$\frac{1}{2}\epsilon_{ijk}\int_{\mathcal{S}}H^i dx^j\wedge dx^k\equiv\int_{\partial\mathcal{S}}A_k dx^k\,, \tag{26}$$

where the integration goes over a surface in the transverse plane which includes the position of the dislocation. For the considered solution of elasticity equations (21) we represent the right hand side of this expression as follows

$$\int_{\partial\mathcal{S}}A_k dx^k=b^iK_i^{(0)}+\frac{1}{a}\beta_{ijk}\int_{\partial\mathcal{S}}u^{jk}dx^i \tag{27}$$

The first term in this expression gives the following singular contribution to magnetic field:

$$H^k_{\rm sing}(\boldsymbol{x})\approx b^iK_i^{(0)}\int_{l^0}dy^k(s)\delta^{(3)}(x-y(s)), \tag{28}$$

where the integration over y goes along the dislocation axis l^0. One can check that the solutions of elasticity equations give $u^{jk}\sim 1/r$ at $r\to\infty$. Therefore, the integral along the circle $\mathcal{C}_r\equiv\partial\mathcal{S}$ at $r\to\infty$ (with the dislocation at its center) in the second term of Eq. (27) gives finite contribution to the normalized total flux of the singular gauge field $\boldsymbol{H}_{\rm sing}$:

$$\hat{\Phi}(r)=\frac{\Phi(r)}{\Phi_0}=\frac{1}{2\pi}\int_{\mathcal{C}_r}A_k dX^k\,, \tag{29}$$

where

$$\Phi_0=2\pi \tag{30}$$

is the elementary flux (in out units the electric charge is unity $e=1$). At the same time the function $\hat{\Phi}(\infty)-\hat{\Phi}(r)$ takes its maximum at $r=0$ and decreases fast out of the core of the dislocation.

In the considered crystals there exist several exceptional vectors $\boldsymbol{G}_i$ ($i=0,1,2,...$), which generate the symmetry of Brillouin zone, i.e. momenta $\boldsymbol{k}$ and $\boldsymbol{k}+\boldsymbol{G}_i$ are equivalent. The unperturbed Fermi point is directed along $\boldsymbol{G}_0$ and is also defined up to the transformations $\boldsymbol{K}^{(0)}\to\boldsymbol{K}^{(0)}+\boldsymbol{G}_i$. This corresponds to the change of the magnetic flux by

$$\Delta\hat{\Phi}=\boldsymbol{b}\cdot\boldsymbol{G}_i=2\pi N\,,\qquad N\in\mathbb{Z}\,. \tag{31}$$

Such a change of the magnetic flux is unobservable for Weyl fermions and Eq. (31) is thus posing certain restrictions on the choice of the Burgers vectors. For example, for the layered hexagonal structure of Na and Bi atoms in the compound Na_3Bi we have

$$\boldsymbol{G}_1=\frac{4\pi}{3a}\hat{\boldsymbol{x}},\quad \boldsymbol{G}_2=\frac{4\pi}{3a}(\frac{1}{2}\hat{\boldsymbol{x}}+\frac{\sqrt{3}}{2}\hat{\boldsymbol{y}}),$$
$$\boldsymbol{G}_3=\frac{4\pi}{3a}(\frac{1}{2}\hat{\boldsymbol{x}}-\frac{\sqrt{3}}{2}\hat{\boldsymbol{y}}),\quad \boldsymbol{G}_0=\zeta\frac{4\pi}{3a}\hat{\boldsymbol{z}}. \tag{32}$$

Here a is the interatom distance within each layer in the plane orthogonal to $\boldsymbol{G}_0\parallel\boldsymbol{K}^{(0)}$ and the material parameter ζ determines the interlayer distance. Due to the hexagonal (honeycomb) structure of the Na_3Bi layers in xy plane, we may construct the Burgers vectors similarly to the case of graphene [34] which has also the hexagonal

structure. Condition (31) gives us the following general expression for the Burgers vectors:

$$\boldsymbol{b} = \sum_i N_i \boldsymbol{m}_i \tag{33}$$

where $N_i \in \mathbb{Z}$. The vectors $\boldsymbol{m}_i$

$$\begin{aligned}
\boldsymbol{m}_0 &= \frac{3a}{2\zeta}\hat{\boldsymbol{z}}\,,\\
\boldsymbol{m}_1 &= -\boldsymbol{l}_1 + \boldsymbol{l}_2 \equiv \frac{3a}{2}\hat{\boldsymbol{x}} + \frac{\sqrt{3}a}{2}\hat{\boldsymbol{y}}\,,\\
\boldsymbol{m}_2 &= \boldsymbol{l}_3 - \boldsymbol{l}_2 \equiv -\sqrt{3}a\hat{\boldsymbol{y}}\,,\\
\boldsymbol{m}_3 &= \boldsymbol{l}_1 - \boldsymbol{l}_3 \equiv -\frac{3a}{2}\hat{\boldsymbol{x}} + \frac{\sqrt{3}a}{2}\hat{\boldsymbol{y}}\,,
\end{aligned} \tag{34}$$

are constructed from the nearest-neighbor vectors of the NaBi honeycomb lattice in the transverse planes of Na_3Bi:

$$\begin{aligned}
\boldsymbol{l}_1 &= -a\,\hat{\boldsymbol{x}},\\
\boldsymbol{l}_2 &= a\left(\frac{1}{2}\hat{\boldsymbol{x}} + \frac{\sqrt{3}}{2}\hat{\boldsymbol{y}}\right),\\
\boldsymbol{l}_3 &= a\left(\frac{1}{2}\hat{\boldsymbol{x}} - \frac{\sqrt{3}}{2}\hat{\boldsymbol{y}}\right).
\end{aligned} \tag{35}$$

For a screw dislocation perpendicular to the layers of Na_3Bi the displacement vector is given by Eq. (17). The only nonzero components of the corresponding deformation tensor (19) are

$$u^{3a}(\boldsymbol{x}_\perp) \equiv u^{a3}(\boldsymbol{x}_\perp) = \frac{b_3 \epsilon^{3ab} x^b_\perp}{4\pi \boldsymbol{x}^2_\perp}\,, \tag{36}$$

and the emergent electromagnetic field (21) is given by

$$A_i = -\nabla_i(\boldsymbol{u}\boldsymbol{K}) + \frac{\beta}{a}u^{3i} + \frac{\beta'}{a}\epsilon_{3ij}u^{3j}\,, \quad A_0 = 0\,, \tag{37}$$

with some material-dependent constants β and β'. Notice that our expression (37) differs from Eq. (25) of Ref. [35]. Equation (37) leads to the following expression for the (normalized) magnetic flux of the emergent magnetic field $\boldsymbol{H}$:

$$\hat{\Phi}(\infty) = \frac{\boldsymbol{K}^{(0)}\boldsymbol{b}}{2\pi} + \frac{\beta}{4\pi a}b_3 \tag{38}$$

Notice, that in the modeling case, when the emergent $U(1)$ field is given by Eq. (25), the magnetic flux $\hat{\Phi}(\infty)$ is given by the same expression. For example, in Na_3Bi the value of $\boldsymbol{K}^{(0)} \approx 0.26\frac{\pi}{a_z}\hat{z}$, where a_z is the lattice spacing in z direction [1, 45]. The value of $b_3 = Na_z$ is proportional to a_z. Therefore, the topological contribution to magnetic flux of the dislocation is $\frac{\boldsymbol{K}^{(0)}\boldsymbol{b}}{2\pi} \approx \frac{0.26\pi N}{2\pi} \approx 0.13\,N$. Following an analogy to graphene, where Gruneisen parameter $\beta \sim 2$ we may roughly estimate the second term in Eq. (38) as $\sim 0.2\,N$. Then the emergent magnetic flux incident at the dislocation, presumably, reaches the value of 2π at $N \sim 30$.

As it was mentioned above we may neglect the zero component of the emergent electromagnetic field A_0 at large distances $r \gg a$, where the elasticity theory works. However, such a potential may be present within the dislocation core because of the essential change in the microphysics. Thus we assume the existence of either repulsive or attractive potential

$$A_0(\boldsymbol{x}_\perp) = v_F \nu^{-1/3}\phi(\boldsymbol{x}_\perp)\,, \tag{39}$$

at the dislocation core and we neglect possible appearance of such potential far from the dislocation.

IV. EMERGENT GRAVITY AROUND THE DISLOCATION

Momentum of quasiparticles that are described by the action of Eq. (8) should be much smaller than $1/a$. At the same time the emergent gauge field $\boldsymbol{A}$ within the dislocation core may be as large as $\sim 1/a$. Therefore, the contribution of emergent gravity to Eq. (8) is always small compared to the contribution of the emergent gauge field. Nevertheless, for the completeness in this section we briefly consider emergent gravity around the dislocation. Let us represent the action for the right-handed fermion in the following way:

$$\begin{aligned}
S_R &= \int d^3x\,dt\,\bar{\Psi}(x,t)\Big[|\boldsymbol{e}(x)|e^0_0(x)i\partial_t\\
&\quad -|\boldsymbol{e}(x)|e^k_a(x)\sigma^a \circ (\hat{P}_k - A_k)\Big]\Psi(x,t)\\
&= \int d^3x\,dt\,\bar{\tilde{\Psi}}(x,t)\Big[i\partial_t - \mathcal{H}^{(R)}\Big]\tilde{\Psi}(x,t),
\end{aligned} \tag{40}$$

where $\hat{P}_k = -i\nabla_k$, $\tilde{\Psi} = \sqrt{|\boldsymbol{e}(x)|e^0_0(x)}\,\Psi$, $a = 0,1,2,3$ and $k = 1,2,3$. The one-particle Hamiltonian is given by

$$\mathcal{H}^{(R)} = f^k_a(x)\sigma^a \circ (\hat{P}_k - A_k), \tag{41}$$

where

$$f^k_a(x) = \frac{e^k_a(x)}{e^0_0(x)}\,. \tag{42}$$

We used here the following chain of relations:

$$\int d^3x\,dt\,\left\{\frac{\bar{\widetilde{\Psi}}(x,t)}{\sqrt{|\boldsymbol{e}(x)|e_0^0(x)}}\,|\boldsymbol{e}(x)|e_a^k(x)\sigma^a\partial_i\frac{\widetilde{\Psi}(x,t)}{\sqrt{|\boldsymbol{e}(x)|e_0^0(x)}}-\left[\partial_i\frac{\bar{\widetilde{\Psi}}(x,t)}{\sqrt{|\boldsymbol{e}(x)|e_0^0(x)}}\right]\,|\boldsymbol{e}(x)|e_a^k(x)\sigma^a\frac{\widetilde{\Psi}(x,t)}{\sqrt{|\boldsymbol{e}(x)|e_0^0(x)}}\right\}$$
$$=\int d^3x\,dt\,\left\{\bar{\widetilde{\Psi}}(x,t)\frac{1}{|\boldsymbol{e}(x)|e_0^0(x)}\,|\boldsymbol{e}(x)|e_a^k(x)\sigma^a\partial_i\widetilde{\Psi}(x,t)-\left[\partial_i\bar{\widetilde{\Psi}}(x,t)\right]\,|\boldsymbol{e}(x)|e_a^k(x)\sigma^a\frac{1}{|\boldsymbol{e}(x)|e_0^0(x)}\widetilde{\Psi}(x,t)\right\} \quad (43)$$
$$=\int d^3x\,dt\,\left\{\bar{\widetilde{\Psi}}(x,t)f_a^k(x)\,\sigma^a\partial_i\widetilde{\Psi}(x,t)-\left[\partial_i\bar{\widetilde{\Psi}}(x,t)\right]\sigma^a f_a^k(x)\widetilde{\Psi}(x,t)\right\}\equiv 2\int d^3x\,dt\,\bar{\widetilde{\Psi}}(x,t)\left[f_a^k(x)\,\sigma^a\circ\partial_i\right]\widetilde{\Psi}(x,t).$$

We represent $f_a^k(x)$ as follows

$$f_a^k(x)\approx v_F\left[\hat{f}_a^\mu-\hat{f}_b^\mu\delta e_a^b(x)\right]$$
$$f_0^k(x)\approx -v_F\hat{f}_b^\mu\delta e_0^b(x),\quad a,b,k=1,2,3\,, \quad (44)$$

where the expressions for the small variations of the vierbein field δe_a^μ can be read off from Eq. (20).

The one-particle Hamiltonian for the right-handed fermions in the presence of a dislocation along the z axis is given by

$$\mathcal{H}^{(R)}=v_F\nu^{2/3}\sigma^3\hat{p}_3-v_F\nu^{2/3}\sum_{a=0}^{3}\sigma^a\delta e_a^3\hat{p}_3$$
$$+v_F\nu^{-1/3}\mathcal{H}_\perp^{(R)}\,, \quad (45)$$

where the transverse part of the Hamiltonian is

$$\mathcal{H}_\perp^{(R)}\approx\sum_{a=1,2}\left[\sigma^a\Big(\hat{p}_a-A_a(\boldsymbol{x}_\perp)\Big)-\sum_{k=1,2}\sigma^a\delta e_a^k(\boldsymbol{x}_\perp)\circ\hat{p}_k\right]$$
$$+\phi(x,y)-\sigma^3A_3(\boldsymbol{x}_\perp) \quad (46)$$
$$-\sum_{k=1,2}\left[\sigma^3\delta e_3^k(\boldsymbol{x}_\perp)+\delta e_0^k(\boldsymbol{x}_\perp)\right]\circ\hat{p}_k\,.$$

In a general form, the dislocation-induced deformations of the vielbein field δe_a^μ in the Hamiltonian (45), (46) can be expressed via components tensor γ_{jkl}^i of Eq. (20) and the relations given in Eqs. (42) and (44). However, in certain symmetric cases the form of the Hamiltonian may be simplified. Consider, for example, the case, when the screw dislocation is directed along the z axis of the Na_3Bi atomic lattice (or, equivalently, along the vector $\boldsymbol{K}^{(0)}$). Then, one can write the following expression for the deformations of the veilbein:

$$\delta e_a^k=\gamma_1K^{akj}u^{3j}+\gamma_2\widetilde{K}^{akj}u^{3j},\qquad a,k=1,2, \quad (47)$$
$$\delta e_3^k=\gamma_3\epsilon_{3kj}u^{3j}+\gamma_4u^{3k},\qquad k=1,2, \quad (48)$$
$$\delta e_k^3=\gamma_5u^{3k}+\gamma_6\epsilon_{3kj}u^{3j}+u^{3k},\qquad k=1,2, \quad (49)$$
$$\delta e_3^3=0, \quad (50)$$
$$\delta e_0^k=0,\qquad k=1,2. \quad (51)$$

Here we have used the fact that the only nonzero components of the tensor of elastic deformations (19) are $u^{3i}=u^{i3}$ with $i=1,2$ given in Eq. (36). Moreover, we took into account that the dislocation is directed along the z axis which is perpendicular to layers of honeycomb lattices formed by Na and Bi atoms in the transverse (x,y) plane. The requirement to respect the C_3 rotational symmetry of the honeycomb lattice in the (x,y) plane allows us to define two tensors from the nearest-neighbor vectors (35):

$$K^{ijk}=-\frac{4}{3a^3}\sum_{b=1,2,3}l_b^il_b^jl_b^k \quad (52)$$

$$\widetilde{K}^{ijk}=-\frac{4}{3a^3}\sum_{b=1,2,3}l_b^il_b^jl_b^m\epsilon_{3mk} \quad (53)$$

which enter Eq. (47) with material-dependent prefactors γ_1 and γ_2, respectively. The only nonzero elements of these tensors are:

$$-K^{111}=K^{122}=K^{212}=K^{221}=1\,,$$
$$\widetilde{K}^{112}=\widetilde{K}^{121}=\widetilde{K}^{211}=-\widetilde{K}^{222}=1\,. \quad (54)$$

The tensor (52) was first introduced in Refs. [28, 29]. The appearance of the second tensor structure (53) in Eq. (47) is a nontrivial fact because the tensor $\widetilde{K}^{ijk}$ is not invariant under P-parity transformation of the 3d space. The P-parity odd part is justified, however, by the chiral property of the screw dislocation, because the left-handed screws and right-handed screws are not equivalent as they cannot be superimposed on each other with the help of rotations only. Therefore, P-parity odd terms may appear in the Hamiltonian.

Similar arguments lead to appearance of four other material-dependent terms in Eqs. (48) and (50) with parameters $\gamma_3,\ldots,\gamma_6$. Equation (51) originates from the supposition that the dislocation does not break T invariance so that all components of the vielbein involving one temporal and one spatial components must be zero. Notice that the deformation of the e_0^0 does not enter the Hamiltonian (41) because $f_0^0\equiv 1$ according to Eq. (42).

One can see, that even in this relatively simple case, the expressions in Eqs. (47)-(51) contain six phenomenological parameters γ_i, and the resulting Hamiltonian $\mathcal{H}^{(R)}$, given in Eqs. (46) and (45), is rather complicated.

V. FERMION ZERO MODES PROPAGATING ALONG THE DISLOCATION

In this section we show that the dislocations in a Dirac semimetal hosts a massless (quasi)fermion mode which propagates along the dislocation with the Fermi velocity. This fermionic mode is a zero mode of the transverse

Hamiltonian (46). The appearance of the propagating mode localized in the vicinity of the dislocation is also known to emerge in topological insulators with lattice dislocations [44].

Let us neglect the emergent gravity due to its weakness and concentrate first on the case of screw dislocation, when $A_3 = 0$. We may apply the gauge transformation, which brings the gauge field to the form

$$A_i = \epsilon_{3ij}\partial_j f(\boldsymbol{x}_\perp)\,, \tag{55}$$

where f is a certain function of transverse coordinates. Then the Hamiltonian (41) becomes as follows:

$$\mathcal{H}^{(R)} = v_F\nu^{2/3}\sigma^3\hat{p}_3 + v_F\nu^{-1/3}\mathcal{H}_\perp^{(R)} \tag{56}$$

with

$$\mathcal{H}_\perp^{(R)} \approx \phi(x_\perp) + \sum_{a=1,2}\Big(\sigma^a\hat{p}_a + \sum_{b=1,2}\sigma^a\epsilon_{ab}\partial_b f(x_\perp)\Big). \tag{57}$$

The zero modes of the transverse Hamiltonian $\mathcal{H}_\perp^{(R)}$ are defined as solution of the equation

$$\mathcal{H}_\perp^{(R)}\psi = 0\,. \tag{58}$$

Next, we represent $\psi = e^{-\sigma^3 f}\widetilde{\psi}$ and rewrite the Hamiltonian in the polar coordinates r, θ in the transverse $\boldsymbol{x}_\perp = (x_1, x_2)$ using

$$x_1 = r\cos\theta, \quad x_2 = r\sin\theta, \tag{59}$$

$$\hat{p}_r = -i\partial_r, \qquad \hat{p}_\theta = -\frac{i}{r}\partial_\theta, \tag{60}$$

and the radial sigma matrices:

$$\sigma^r = \begin{pmatrix} 0 & e^{-i\theta} \\ e^{i\theta} & 0 \end{pmatrix}, \quad \sigma^\theta = \begin{pmatrix} 0 & -ie^{-i\theta} \\ ie^{i\theta} & 0 \end{pmatrix} \tag{61}$$

Then equation for the function $\widetilde{\psi}$ is $\widetilde{\mathcal{H}}_\perp^{(R)}\widetilde{\psi} = 0$, where

$$\widetilde{\mathcal{H}}_\perp^{(R)} \approx \phi(r,\theta) + \sigma^r\hat{p}_r + \sigma^\theta\hat{p}_\theta \tag{62}$$

Next, we have

$$\widetilde{\mathcal{H}}_\perp^{(R)} = \sigma^1\begin{pmatrix} e^{i\theta}\mathcal{H}_+^{(R)} & \phi(r,\theta) \\ \phi(r,\theta) & e^{-i\theta}\mathcal{H}_-^{(R)} \end{pmatrix}, \quad \mathcal{H}_-^{(R)} = \left[\mathcal{H}_+^{(R)}\right]^\dagger \tag{63}$$

with

$$\mathcal{H}_\pm^{(R)} \approx \hat{p}_r \pm i\hat{p}_\theta \tag{64}$$

In the absence of the electric potential $\phi(r,\theta)$ the zero modes (if they exist) have a definite value of the spin projection $s = \pm 1/2$ on the z axis. At large r the corresponding coordinate parts of their wave functions satisfy the relations

$$(\hat{p}_r \pm i\hat{p}_\theta)\widetilde{\psi}_\pm^{(m)} = 0\,. \tag{65}$$

Next, we chose

$$f(r,\theta) = \int_0^r \hat{\Phi}(r,\theta)\frac{dr}{r}\,, \tag{66}$$

so that the only nonzero component of the gauge potential (55) gets the following form:

$$A_\theta = \frac{\hat{\Phi}(r,\theta)}{r}\,. \tag{67}$$

The axial symmetry of the problem implies that at large distances r the function $\hat{\Phi}(r,\theta)$ is independent of the polar angle θ. Therefore, at large r the function $\hat{\Phi}(r)$ is the magnetic flux within the circle S_r of radius r:

$$\hat{\Phi}(r) = \frac{1}{2\pi}\int_{S_r}\frac{1}{2}\epsilon_{ijk}dx^j \wedge dx^k H^i(x,y)\,, \tag{68}$$

where the surface S_r belongs to the plane which is orthogonal to the dislocation. We come to the following solutions of Eq. (58) for the zero modes [42]:

$$\psi_\pm^{(m)}(r,\theta) \sim r^m e^{\pm im\theta \mp \int_0^r \hat{\Phi}(r,\theta)\frac{dr}{r}}\,, \tag{69}$$

where the integer m is the angular quantum number.

The solutions (69) are localized in a small vicinity of the dislocation core provided the angular quantum number satisfy the following condition

$$m - 2s\hat{\Phi} < -1, \qquad \hat{\Phi} = \lim_{r\to\infty}\hat{\Phi}(r,\theta)\,, \tag{70}$$

and in this case the corresponding probability distribution is convergent at large r:

$$\int_\xi^\infty r dr d\theta |\psi|^2 = 1\,. \tag{71}$$

Notice that ξ is of the order of the lattice constant a.

In addition, there exist two solutions of Eq. (65), which may not be normalized and which have their maxima at the dislocation core provided

$$m = [2s\hat{\Phi}(\infty)], \tag{72}$$

where $[2s\hat{\Phi}]$ is the integer part of $2s\hat{\Phi}$, which is the maximal integer number that is not larger than $2s\hat{\Phi}$.

The probability distributions of the considered solutions are convergent at small r for $m \geq 0$. Therefore, in the absence of both the vielbein and the electric potential, the zero modes that are not singular at $r \to 0$ and are not localized on the boundaries of the system, should satisfy $0 \leq m \leq 2s\hat{\Phi}(\infty)$. Such modes exist for $s\hat{\Phi}(\infty) > 0$ and are enumerated by the values of orbital momentum

$$m = 0, ..., [2s\hat{\Phi}], \tag{73}$$

We neglected in this derivation the potential ϕ. However, it is localized at the dislocation. Therefore, the zero modes in the presence of electric potential (if they

exist) have the form of Eq. (69) at $r \gg a$. Recall, that Eq. (8) works for the momenta of quasiparticles much smaller, than $1/a$. Therefore, the solutions of Eq. (58) localized at the dislocations, presumably, do not represent physical zero modes. The only solution that remains is the one with

$$m = [2s\hat{\Phi}], \quad s = \frac{1}{2}\text{sign}\,\hat{\Phi} \tag{74}$$

Fortunately, the field ϕ cannot affect the energy of this solution because the probability density corresponding to this solution of Eq. (65) is dominated by the distances far from the dislocation core, so that we can neglect completely the region of the dislocation core. The vielbein for this solution also gives small corrections compared to the contribution of emergent magnetic field. Therefore, the strong gravity and the potential ϕ at $r \sim \xi$ cannot affect the main properties of this solution: it certainly survives as the zero mode and still has the definite value of the projection of spin to the z axis.

In the case of edge or mixed dislocation we should take into account the appearance of a nonzero third component of the emergent gauge field:

$$A_3(\boldsymbol{x}_\perp) \approx \frac{1}{r^2}\left(\beta_1 \boldsymbol{b}_\perp \boldsymbol{x}_\perp + \beta_2 \epsilon_{3ij} b^i_\perp x^j_\perp\right). \tag{75}$$

Then far from the dislocation core one gets

$$\widetilde{\mathcal{H}}^{(R)}_\perp = \sigma^1 \begin{pmatrix} e^{i\theta}\mathcal{H}^{(R)}_+ & \nu A_3(r,\theta) \\ -\nu A_3(r,\theta) & e^{-i\theta}\mathcal{H}^{(R)}_- \end{pmatrix} \tag{76}$$

One can check, that the first order perturbative correction to the eigenenergy of the zero mode (69) due to the presence of A_3 vanishes completely. Next order corrections may be nonzero, in principle, but for the mode with $m = [2s\hat{\Phi}(\infty)]$ those corrections may be neglected because all integrals are dominated by the regions with $r \to \infty$ while $A_3 \sim 1/r$.

Thus we come to the conclusion, that the only zero mode existing around the dislocation is the one with

$$m = [2s\hat{\Phi}(\infty)]\,, \qquad s = \frac{1}{2}\text{sign}\,\hat{\Phi}(\infty)\,. \tag{77}$$

The zero mode (69), (77) of the transverse Hamiltonian $\mathcal{H}^{(R)}_\perp$ corresponds to the zero mode of the full Hamiltonian $\mathcal{H}^{(R)}$ provided the longitudinal momentum is zero $p_3 = 0$. At the same time it corresponds to a linear branch of spectrum of the full Hamiltonian $\mathcal{H}^{(R)}$ with the corresponding dispersion law:

$$\mathcal{E}^{(R)} \approx v_F \nu^{2/3} \text{sign}(\hat{\Phi})\, p_3\,. \tag{78}$$

This branch crosses zero energy level at $p_3 = 0$.

Similar considerations can also be applied to the left-handed Hamiltonian $\mathcal{H}^{(L)}$, where the only physical zero mode of the corresponding transverse part $\mathcal{H}^{(L)}_\perp$ is

$$\psi^{(m)}_{2s}(r,\theta) \sim r^m e^{i2sm\theta - 2s\int_0^r \hat{\Phi}(r)\frac{dr}{r}} \tag{79}$$

with the quantum numbers

$$m = [2s\hat{\Phi}], \quad s = \frac{1}{2}\text{sign}\,\hat{\Phi}\,. \tag{80}$$

This mode corresponds to the branch of spectrum with the dispersion

$$\mathcal{E}^{(L)} \approx -v_F \nu^{2/3} \text{sign}(\hat{\Phi})\, p_3\,. \tag{81}$$

The right-handed and left-handed fermionic modes propagate along the dislocation with the velocity

$$v_R = -v_L = v_F \nu^{2/3} \text{sign}(\hat{\Phi})\,, \tag{82}$$

which is nothing but the corresponding component of the anisotropic Fermi velocity. Thus, the right-handed massless quasiparticle propagates up or down along the dislocation depending on the sign of the flux Φ. The left-handed mode always propagates in the opposite direction compared to the right-handed mode.

Notice that Eqs. (78) and (81) were derived in the assumption that the magnetic fluxes of the emergent magnetic field for the right-handed Φ_R and the left-handed Φ_L quasiparticles are the same, $\Phi_R = \Phi_L \equiv \Phi$. However, if in a Dirac semimetal the constants β_{ijk} differ for the left-handed and the right-handed fermions, then the corresponding gauge fields (21) are also different, and in this case the magnetic flux entering Eq. (78) will be different from the flux in Eq. (81).

VI. CHIRAL ANOMALY IN DIRAC SEMIMETALS ALONG THE DISLOCATION

In the presence of external electric field $\boldsymbol{E}$ the states that correspond to the described above zero modes flow in the correspondence with the following equation:

$$\langle \dot{p}_3 \rangle = E_3\,. \tag{83}$$

Now let us take into account, that the studied model has the infrared cutoff $1/\xi_0$, where $\xi_0 \gg a$. Then the zero modes of $\mathcal{H}^{(R)}_\perp$ and $\mathcal{H}^{(L)}_\perp$, and the corresponding branches of fill spectrum of propagating modes of the full Hamiltonians $\mathcal{H}^{(R)}$ and $\mathcal{H}^{(L)}$ obey the following properties:

1. The propagating fermion modes are not localized at the dislocation core. Instead, the region of space around the dislocation of size ξ_0 dominates, where $1/\xi_0$ is the infrared cutoff of the theory.

2. The propagating fermion modes have the definite value of the spin projection on the dislocation axis: $s = \frac{1}{2}\text{sign}\,\hat{\Phi}$. The corresponding branch of spectrum for right- and left-handed fermions is given by, respectively, the following dispersion relations:

$$v_{R/L}(p_3) = \pm v_F \nu^{2/3} 2s\, p_3\,. \tag{84}$$

3. The propagating mode appears for any dislocations including those ones, in which the magnetic flux $\hat{\Phi}$ is smaller than unity.

The total production of the right-handed quasiparticles per unit length of the dislocation is given by:

$$\dot{q}_R = \frac{\boldsymbol{E}\boldsymbol{n}}{2\pi}\mathrm{sign}\,\hat{\Phi}, \tag{85}$$

where the unit vector $\boldsymbol{n}$ is directed along the dislocation. In the following we assume for simplicity, that the signs of the emergent fluxes $\hat{\Phi}$ experienced by the right-handed and the left-handed fermions coincide in the Dirac semimetal. Therefore, the production of the left-handed quasiparticles in Dirac semimetal is given by

$$\dot{q}_L = -\dot{q}_R\,. \tag{86}$$

Production of the quasiparticles may be written as the anomaly in their currents

$$j^\mu_L = |\boldsymbol{e}(x)|J^\mu_L(x)\,, \qquad j^\mu_R = |\boldsymbol{e}(x)|J^\mu_R(x)\,, \tag{87}$$

$$\boldsymbol{j} = \boldsymbol{j}_R + \boldsymbol{j}_L\,, \qquad \boldsymbol{j}_5 = \boldsymbol{j}_R - \boldsymbol{j}_L\,, \tag{88}$$

where the covariant currents are defined according to Eqs. (11) and (12). This anomaly in local form may be written as as follows:

$$\langle\partial_\mu \boldsymbol{j}^\mu_5(x)\rangle = \frac{\boldsymbol{E}\boldsymbol{n}}{\pi}\,f_0(x_\perp)\,\mathrm{sign}\,\hat{\Phi}\,, \tag{89}$$

$$f_0(x_\perp) = \frac{\exp\left(-|x_\perp|/\xi_0\right)\left(\frac{x_\perp}{\xi_0}\right)^{-2(|\hat{\Phi}|-[|\hat{\Phi}|])}}{2\pi\xi_0^2\Gamma(-2|\hat{\Phi}|+2[|\hat{\Phi}|]+2)}\,. \tag{90}$$

Here the function $f_0(r)$ is normalized in such a way, that $2\pi\int rdrf_0(r) = 1$ and $1/\xi_0$ has the meaning of infrared cutoff of the theory. The factor $\exp\left(-|x_\perp|/\xi_0\right)$ appears as the infrared regulator. We imply, that the size of the semimetal sample is much larger than the infrared cutoff ξ_0, while ξ_0 is much larger than the size of the dislocation core $\xi \sim a$, $\xi_0 \gg \xi$. Thus the chiral anomaly due to the zero mode with $m = [|\hat{\Phi}|]$ is localized within the tube of size ξ_0 centered at the dislocation.

It is worth mentioning, that for a single dislocation, when for some reasons the contributions to the emergent magnetic flux of the dislocation due to β_{ijk} in Eq. (21) may be neglected, the typical values of the Burgers vector are such that $|\hat{\Phi}| < 1$. Therefore, according to Eqs. (77) and (80), for a single dislocation the zero mode corresponds to $m = 0$.

We may rewrite the expression for chiral anomaly caused by single dislocation in Dirac semimetal as follows

$$\partial_\mu\langle j^\mu_5(x)\rangle = \frac{\boldsymbol{E}\boldsymbol{B}}{2\pi^2}\,, \tag{91}$$

where the effective magnetic field $\boldsymbol{B}$ responsible for the chiral anomaly is given by

$$\boldsymbol{B}(\boldsymbol{x}_\perp) = 2\pi\boldsymbol{n}\,f_0(\boldsymbol{x}_\perp)\,\mathrm{sign}\,\hat{\Phi}\,. \tag{92}$$

In the presence of the chiral chemical potential μ_5 in the Dirac semimetal the chiral magnetic effect appears:

$$j^k(x) = \frac{2}{2\pi}\int_0^{\mu_5/(v_F\nu^{2/3})} dp_3|\boldsymbol{e}|\,e^k_a\Big[\psi^{(m)}_s(x)\Big]^+\sigma^a\psi^{(m)}_s(x) \tag{93}$$

Here $\psi^{(m)}_s(x)$ is the wave function of the mentioned above zero mode. As we have mentioned above, for the integrals involving bi-fermionic variables the region outside the dislocation core dominates, so that we have for Eq. (93):

$$\boldsymbol{j}(x) \approx \frac{2\mu_5\,\boldsymbol{n}}{2\pi}\,\mathrm{sign}(\hat{\Phi})\,|\psi^{(0)}(x)|^2 \approx \frac{\mu_5}{2\pi^2}\,\boldsymbol{B}(x_\perp)\,. \tag{94}$$

This current is concentrated in the wide region around the dislocation.

It is worth mentioning, that the above consideration refers only to the branches of spectrum, which are described by the low energy effective field theory. At the same time the pumping of the quasiparticles from vacuum may occur in the presence of electric field on another branches of spectrum as well. Ideally, this pumping process should be considered using microscopic theory and is out of the scope of the present paper.

VII. THE CASE OF DISLOCATION DIRECTED ARBITRARILY

In this section we consider the dislocation directed arbitrarily. Without loss of generality we may consider the dislocation directed along an axis, which belongs to the (yz) plane. The angle between the dislocation and the z axis is denoted by φ. Let us rotate the reference frame in such a way, that the z axis is directed along the dislocation. In the new reference frame tensor $\hat{f}$ has the form:

$$\hat{f} = \begin{pmatrix} \nu^{-1/3} & 0 & 0 \\ 0 & \nu^{-1/3}\cos\varphi & \nu^{-1/3}\sin\varphi \\ 0 & -\nu^{2/3}\sin\varphi & \nu^{2/3}\cos\varphi \end{pmatrix} \tag{95}$$

Let us apply transformation of spinors $\psi \to e^{i\frac{\alpha}{2}\sigma^3}$ with $\mathrm{tg}\,\alpha = \nu\,\mathrm{tg}\,\varphi$. In the transformed frame the tensor $\hat{f}$ is modified:

$$\hat{f} = \begin{pmatrix} \nu^{-1/3} & 0 & 0 \\ 0 & \nu^{1/3}\sqrt{\nu^{-4/3}\cos^2\varphi + \nu^{2/3}\sin^2\varphi} & \frac{(1-\nu^2)\sin 2\varphi}{2\nu\sqrt{\nu^{-4/3}\cos^2\varphi+\nu^{2/3}\sin^2\varphi}} \\ 0 & 0 & \frac{1}{\sqrt{\nu^{-4/3}\cos^2\varphi+\nu^{2/3}\sin^2\varphi}} \end{pmatrix} \quad (96)$$

The one-particle Hamiltonian for the right-handed fermions becomes as follows

$$\mathcal{H}^{(R)} = v_F \hat{f}_3^3 \sigma^3 \hat{p}_3 + v_F \hat{f}_3^2 \sigma^2 \hat{p}_3 + v_F \hat{f}_1^1 \mathcal{H}_\perp^{(R)} \quad (97)$$

with

$$\mathcal{H}_\perp^{(R)} \approx \sigma^1(\hat{p}_1 - A_1) + \frac{\hat{f}_2^2}{\hat{f}_1^1}\sigma^2(\hat{p}_2 - A_2) - \frac{\hat{f}_3^3}{\hat{f}_1^1}\sigma_3 A_3(x_\perp) + \phi(x_\perp) \quad (98)$$

Now we perform the coordinate transformation

$$y \to \frac{\hat{f}_2^2}{\hat{f}_1^1} y\,, \qquad A_y \to \frac{\hat{f}_1^1}{\hat{f}_2^2} A_y\,, \quad (99)$$

and notice that the equation for the zero mode of Hamiltonian $\mathcal{H}_\perp$ becomes the same as that of Section V. Thus we arrive at the expression for the anomaly in quasiparticle current of Eq. (85). The resulting expression for the chiral anomaly in Dirac semimetal is again given by Eq. (91).

The expression for chiral magnetic effect in Dirac semimetal is

$$\boldsymbol{j}(x) \approx \frac{\mu_5}{2\pi^2}\,\boldsymbol{B}(x_\perp). \quad (100)$$

The effective magnetic field $\boldsymbol{B}$ is still given by Eq. (92). In principle, in this case the function $f_0(r,\theta)$ may depend on the polar angle θ due to anisotropy of the atomic lattice structure of the Dirac semimetal in question. However, in qualitative analysis we may disregard this anisotropy and consider it in the form of Eq. (90).

VIII. CHIRAL CHEMICAL DENSITY AROUND DISLOCATION IN PRESENCE OF ELECTRIC FIELD

The Dirac semimetal possesses two cones, each of which hosts one right-handed and one left-handed Weyl fermion. Since the processes operating in these two cones are equivalent, we concentrate on the cone hereafter (taking into account the fact of the degeneracy later).

In the following we work in the adiabatic approximation by assuming that the chiral chemical potential is slowly varying function of space and time. The chiral charge density is:

$$\rho_5 \equiv j_5^0 = \frac{\mu_5^3}{3\pi^2 v_F^3} + \frac{\mu_5}{3v_F^3}\left(T^2 + \frac{\mu^2}{\pi^2}\right), \quad (101)$$

where T is the temperature of the system and v_F is the Fermi velocity which enters the dispersion relation for the chiral fermions.

The evolution of the local chiral density (101) is governed by (i) the dissipation of the chiral charge density, (ii) the spatial diffusion of the chiral charge and (iii) the quantum anomaly which generates the local chiral charge due to quantum effects. The nonconservation of the axial charge can conveniently be written in the following form:

$$\frac{d\rho_5}{dt} + \boldsymbol{\nabla}\boldsymbol{j}_5 = -\frac{\rho_5}{\tau_V} + \frac{1}{2\pi^2}\boldsymbol{B}\boldsymbol{E}\,, \quad (102)$$

where the first term in the right hand side corresponds to the dissipation of the chiral charge with the rate given by the chirality-changing scattering time τ_V while the second term describes the generation of the chiral charge due to the quantum anomaly. The chiral current,

$$\boldsymbol{j}_5 = -D_5 \boldsymbol{\nabla}\rho_5\,, \quad (103)$$

is given by the diffusion of the chiral charge ρ_5 with the corresponding diffusion constant D_5. We assume that the Dirac semimetal has zero usual chemical potential for the Dirac quasiparticles, $\mu = 0$. Moreover, we consider a linear approximation so that the transport effects, which are discussed here, do not generate a nonzero μ. Substituting Eq. (103) into Eq. (102) one gets the following equation for the chiral charge density:

$$\frac{d\rho_5}{dt} = -\frac{\rho_5}{\tau_V} + D_5\Delta\rho_5 + \frac{1}{2\pi^2}\boldsymbol{B}\boldsymbol{E}\,. \quad (104)$$

In the stationary electric field, $d\boldsymbol{E}/dt = 0$, the chiral charge ρ_5 relaxes towards equilibrium $d\rho_5/dt = 0$ at late times $t \gg \tau_V$. The equilibrium chiral charge density is given by a solution of Eq. (104) with the vanishing left hand side. The corresponding density is:

$$\rho_5(x) = \frac{1}{2\pi^2 D_5}\int d^3y\, G^{(3)}(x-y;\lambda)\big(\boldsymbol{B}(y)\cdot\boldsymbol{E}(y)\big), \quad (105)$$

where

$$\left(-\Delta + L_V^{-2}\right) G^{(3)}(\boldsymbol{x}-\boldsymbol{y};\lambda) = \delta(\boldsymbol{x}-\boldsymbol{y})\,, \quad (106)$$

is the three-dimensional Green's function and

$$L_V = \sqrt{D_5\tau_V}\,, \quad (107)$$

is a characteristic length which controls spatial diffusion of the chiral charge.

Working in a linear approximation we consider a weak electric field $\boldsymbol{E}$, so that the chiral imbalance can always be treated as a small quantity, $\mu_5 \ll T$. In the absence of the usual chemical potential μ, one gets from

Eq. (101) the following relation between the chemical potential with the chiral charge density:

$$\mu_5(x) = \frac{3v_F^3}{T^2}\rho_5(x)\,. \tag{108}$$

Thus we see, that there is the nontrivial distribution of chiral chemical potential around the dislocation with the characteristic length L_V.

Notice, that this chiral chemical potential refers to the single Dirac point with a pair of Weyl fermions.

IX. OBSERVATION OF CHIRAL MAGNETIC EFFECT THROUGH THE CONTRIBUTION TO CONDUCTIVITY

The chiral magnetic effect is described by (6) in which the chiral chemical potential is related to the chiral charge density by Eq. (108). Using the equilibrium expression for the chiral charge density (105), we come to the conclusion that the external electric field generates along the dislocation the following electric current

$$\boldsymbol{j}^{\rm CME}(x) = n_D\frac{3v_F^3}{4\pi^4T^2D_5}\boldsymbol{B}(x) \cdot\int d^3y\, G^{(3)}(x-y;L_V)\,(\boldsymbol{B}(y)\cdot\boldsymbol{E}(y))\,. \tag{109}$$

Here $n_D = 2$ is the number of Dirac points. Now let is consider practically interesting case when the dislocation is a strait line centred at the origin, $x_1 = x_2 = 0$ and directed along the x_3 axis. The dislocation induces the intrinsic magnetic field

$$\boldsymbol{B}(x_\perp) = B_z(x_\perp)\boldsymbol{n}\,, \tag{110}$$

which is directed along the $x_3 \equiv z$ axis (here $\boldsymbol{n}$ is the unit vector in z direction). The intrinsic magnetic field is a function of the transverse coordinates $x_\perp = (x_1, x_2)$ which takes nonzero values in a (small) core of the dislocation. In our model approach we consider the field distributed around the dislocation,

$$B_z(x_\perp) = \mathrm{sign}\,\Phi\,\frac{\exp\left(-|x_\perp|/\xi_0\right)\left(\frac{x_\perp}{\xi_0}\right)^{-2(|\hat\Phi|-[|\hat\Phi|])}}{\xi_0^2\Gamma(-2|\hat\Phi|+2[|\hat\Phi|]+2)} \tag{111}$$

with the characteristic length ξ_0 that is much larger than the size ξ of the dislocation core (the latter is of the order of a few lattice spacings a).

This magnetic field obeys $\int d^2x_\perp B(x_\perp) = 2\pi\,\mathrm{sign}\,\Phi$. The total flux Φ of the intrinsic magnetic field is of a geometrical origin and it is a quantity of the order of unity

$$\hat\Phi = \frac{\Phi}{\Phi_0}, \tag{112}$$

in terms of the elementary magnetic flux (30). For the straight dislocation (111) the axial anomaly generates the axial charge which spreads in the semimetal in the transverse directions according to the equilibrium formula (105).

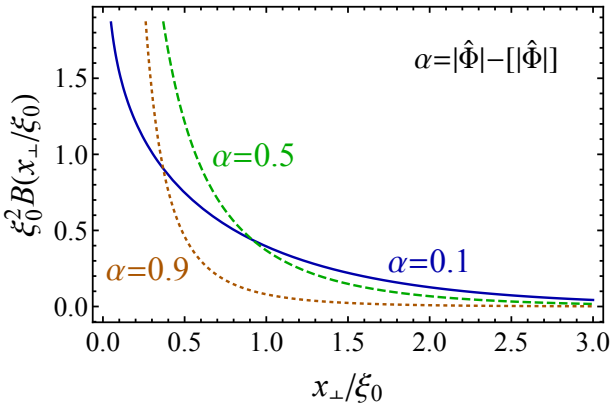

FIG. 3. The effective intrinsic magnetic field $B_z(x_\perp)$ in Eq. (111) vs. the distance from the dislocation core $x_\perp$ plotted for a few values of the fractional part of the absolute value of the normalized flux (112) $\alpha = 0.1,\ 0.5,\ 0.9$.

The distribution of the axial charge around the dislocation is controlled by the the diffusion-related parameter L_V which is typically much larger than the width of the dislocation core and is much smaller, than the length ξ_0 entering Eq. (111). The generated electric current (109) can be written in terms of a local Ohm law:

$$j_i^{\rm CME}(x_\perp) = \sigma_{ij}(x_\perp)E^j\,, \tag{113}$$

where the space-dependent conductivity tensor has the only nonvanishing component

$$\sigma_{zz}(x_\perp) = n_D\frac{3v_F^3}{4\pi^4T^2D_5}B_z(\boldsymbol{x}_\perp) \cdot\int d^2y_\perp\, G^{(2)}(\boldsymbol{x}_\perp-\boldsymbol{y}_\perp;L_V)B_z(\boldsymbol{y}_\perp)\,, \tag{114}$$

while all other components vanish identically. The two-dimensional Green function,

$$G^{(2)}(\boldsymbol{x}_\perp) = \frac{1}{4\pi}K_0\left(x_\perp/L_V\right)\,, \tag{115}$$

is a transverse Green function satisfying a $2d$ analogue of Eq. (106):

$$\left(-\Delta_\perp + L_V^{-2}\right)G^{(2)}(\boldsymbol{x}_\perp-\boldsymbol{y}_\perp;L_V) = \delta(\boldsymbol{x}_\perp-\boldsymbol{y}_\perp). \tag{116}$$

In real Dirac semimetals the value of $\frac{\xi_0}{L_V}$ is around 100. Nevertheless, for the completeness, let us consider the tho limiting cases:

1. Let us first consider the case $L_V \gg \xi_0$, when the characteristic length of diffusion is much larger than the inverse infrared cutoff of the low energy theory. In this case we have

$$G^{(2)}(\boldsymbol{x}_\perp) \approx \frac{1}{4\pi}\log\left(2L_Ve^{-\gamma}/x_\perp\right), \tag{117}$$

where γ is the Euler constant. In the integral in Eq. (114) the values of $|x_\perp| \sim \xi_0$ dominate, and therefore we may take $x_\perp \approx \xi_0$ for our estimation:

$$\sigma_{zz}(x_\perp) = n_D \frac{3v_F^3 |B_z(x_\perp)|}{4\pi^4 T^2 D_5} \frac{\log\left(2L_V e^{-\gamma}/\xi_0\right)}{2} \quad (118)$$

Therefore, the dependence of conductivity on the distance r to the dislocation is given by

$$\sigma_{zz}(x_\perp) \approx n_D \frac{3v_F^3}{4\pi^4 T^2 D_5} \frac{\log\left(2L_V e^{-\gamma}/\xi_0\right)}{2\xi_0^2 \Gamma(2-2\alpha)} \cdot e^{-(x_\perp/\xi_0)} \left(\frac{x_\perp}{\xi_0}\right)^{-2\alpha} . \quad (119)$$

2. Now let us consider the opposite case, $L_V \ll \xi_0$. Then

$$G^{(2)}(\boldsymbol{x}_\perp) \approx L_V^2 \delta^{(2)}(x_\perp) \quad (120)$$

and

$$\sigma_{zz}(x_\perp) = n_D \frac{3L_V^2 v_F^3}{4\pi^4 T^2 D_5} B_z^2(x_\perp) \quad (121)$$

Therefore, in this case the dependence of conductivity on the distance $x_\perp$ to the dislocation axis is stronger:

$$\sigma_{zz}(x_\perp) \approx n_D \frac{3v_F^3}{4\pi^4 T^2 D_5} \frac{L_V^2}{\xi_0^4 [\Gamma(2-2\alpha)]^2} e^{-2(x_\perp/\xi_0)} \left(\frac{x_\perp}{\xi_0}\right)^{-4\alpha} . \quad (122)$$

The total (integrated over the xy slice) current due to the CME has the following form:

$$J_i^{\rm CME} = \sigma_{ij}^{\rm tot} E^j . \quad (123)$$

Equation (109) implies that the conductance tensor $\sigma_{ij}^{\rm tot}$ has only one nonzero component,

$$\sigma_{zz}^{\rm tot} \equiv \int d^2x_\perp \, \sigma_{zz}(x_\perp) = n_D \frac{3v_F^3}{4\pi^4 T^2 D_5} \cdot \int d^2x_\perp d^2y_\perp B_z(\boldsymbol{x}_\perp) G^{(2)}(\boldsymbol{x}_\perp - \boldsymbol{y}_\perp) B_z(\boldsymbol{y}_\perp) \quad (124)$$

$$= n_D \frac{3v_F^3}{4\pi^4 T^2 D_5} \int \frac{d^2k}{(2\pi)^2} \frac{\widetilde{B}_z^2(k)}{k^2 + 1/L_V^2} \quad (125)$$

Here

$$\widetilde{B}(k) = \int d^2x_\perp e^{-ikx_\perp} B(x_\perp) \quad (126)$$

Using the distribution for the magnetic flux around the dislocation (111) we arrive at the following expression for the conductance (124):

$$\sigma_{zz}^{\rm tot} = n_D \frac{3v_F^3}{4\pi^4 T^2 D_5} F\left(|\hat{\Phi}| - [|\hat{\Phi}|], \frac{\xi}{L_V}\right) , \quad (127)$$

where

$$F(\alpha, x) = \int \frac{d^2k}{(2\pi)^2} \frac{\hat{B}_\alpha^2(k)}{k^2 + x^2} , \quad (128)$$

with

$$\hat{B}_\alpha(k) = \frac{1}{\Gamma(2-2\alpha)} \int_0^\infty dz \int_0^{2\pi} d\phi \, z^{1-2\alpha} e^{-ikz\cos\phi - z} = 2\pi \, {}_2F_1\left(1-\alpha, \frac{3}{2} - \alpha, 1; -y^2\right) , \quad (129)$$

Here ${}_2F_1$ is the hypergeometric function. The function $F(\alpha, x)$ is well defined for $\alpha \leq 1$, which is always the case since $\alpha = |\hat{\Phi}| - [|\hat{\Phi}|]$ in Eq. (127). The dependence of the function $F(\alpha, x)$ on α is represented in Fig. 4 for $x = 0.1, 1, 10, 100$.

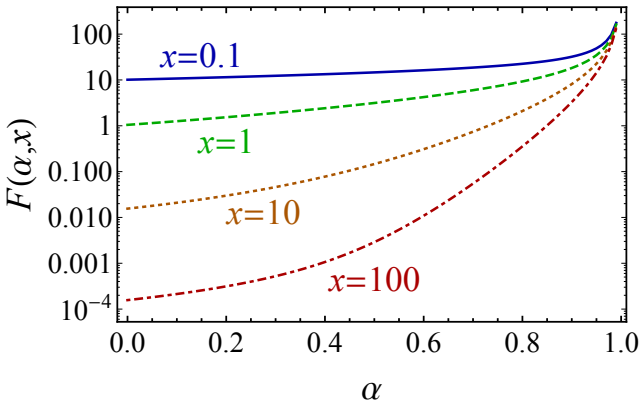

FIG. 4. Function $F(\alpha, x)$ in Eq. (128), where $\alpha = |\hat{\Phi}| - [|\hat{\Phi}|]$ is the fractional part of the absolute value of the normalized flux (112) and $x = \xi_0/L_V$ for $x = 0.1, 1, 10, 100$.

In the two considered above limiting cases the total conductance is given by:

1. For $L_V \gg \xi_0$ we have

$$\sigma_{zz}^{\rm tot} = n_D \frac{3v_F^3}{4\pi^3 T^2 D_5} \log\left(2L_V e^{-\gamma}/\xi_0\right) \quad (130)$$

2. In the opposite case $L_V \ll \xi_0$:

$$\sigma_{zz}^{\rm tot} = n_D \frac{3v_F^3}{4\pi^4 T^2 D_5} \frac{L_V^2}{\xi_0^2} \frac{\sqrt{\pi}\Gamma(3/2-2\alpha)}{(1-2\alpha)\Gamma(2-2\alpha)}, \quad \alpha < 1/2 \quad (131)$$

with $\alpha = |\hat{\Phi}| - [|\hat{\Phi}|]$. For $\alpha \geq 1/2$ and even for the value of α smaller than $1/2$ but close to $1/2$ the above expression does not work, and we should use the exact expression Eq. (127). In practical calculations with $\xi_0 \sim 100 L_V$ the above asymptotic expression gives reasonable results that approximate well the exact expression of Eq. (127) (see Fig. 4) for $\alpha < 0.4$.

X. NUMERICAL ESTIMATES

Now let us estimate a scale of the magnitude of the anomalous contribution to the total conductance of a Dirac semimetal which comes from the chiral anomaly and the (intrinsic) chiral magnetic effect.

We take for a reference the Dirac semimetal Cd_3As_2.The diffusion length of the axial charge for this semimetal was experimentally estimated in Ref. [6] as $L_V \approx 2\times 10^{-6}$m. This quantity turns out to be almost temperature-independent in a wide range of temperatures $T = (50 \sim 300)$ K. A rough estimate of Ref. [7] gives for the relaxation time $\tau_V \sim \tau_{tr} \approx 2\times 10^{-10}$ s. Then from Eq. (107) one finds

$$D_5 = L_V^2/\tau_V \approx 2\times 10^{-2}\mathrm{m}^2/\mathrm{s}\,. \tag{132}$$

Correspondingly the inverse infrared cutoff ξ_0 may be estimated as

$$\xi_0 \sim v_F\tau_V \sim \frac{1}{200}300\cdot 10^6\,\frac{\mathrm{m}}{\mathrm{s}}\cdot 2\times 10^{-10}\mathrm{s} = 3\cdot 10^{-4}\,\mathrm{m} \tag{133}$$

In this estimate we use the value of v_F for Cd_3As_2 that is around 1/200 speed of light. The value of ξ_0 should be compared to the size of the dislocation core

$$\xi \sim 10^{-9}\,\mathrm{m}\,, \tag{134}$$

and to the value of L_V

$$L_V \sim 2\cdot 10^{-6}\,\mathrm{m}\,. \tag{135}$$

Thus we see that in practice the suggested limiting case is indeed realized:

$$L_V \ll \xi_0 \tag{136}$$

and the typical value of $x = \frac{\xi_0}{L_V}$ is $x \sim 100$. At this value of the ratio x the total conductance (127), expressed through the function (128), is very sensitive to (the fractional part $\alpha = |\hat\Phi| - [|\hat\Phi|]$ of) the (normalized) emergent magnetic flux $\hat\Phi$ of the dislocation, as shown in Fig. 4 by the dot-dashed line. From Fig. 4 it is readily seen that while the value of the emergent flux $|\hat\Phi|$ is changing from zero to unity, the total conductance may vary by 6 orders of magnitude! The function F for $x = 100$ takes a unit value $F = 1$ for $|\hat\Phi| \approx 0.85$. Notice that the conductivity diverges at $|\hat\Phi| \to 1$.

Notice, that we used in the present paper the relativistic system of units, in which the only dimensional unit is the electron-volt (eV). Distances are measured in eV^{-1}. Below we estimate the value of conductance induced by the dislocation. Firstly, we give the estimate in relativistic units, where it is expressed through eV or 1/m, where the unit of distance (m) is related to eV^{-1} according to the standard relation $[200\ \mathrm{MeV}]^{-1} \approx 1\ \mathrm{fm} = 10^{-15}$ m. Next, we express the conductance in SI system using the definition of its unit of electric current (A) as Coulomb/s. SI current equal to one Ampere corresponds to the relativistic current equal to $1/(ec)$ in the units of 1/m, where e is the charge of electron (in Coulombs) while c is the speed of light (in m/s).

For the beginning, let us consider the room temperature $T \sim 300\,\mathrm{K} \approx 0.025$ eV. At the same time $D_5/c \approx 6.7\cdot 10^{-11}\mathrm{m} = 6.7\cdot 10^4\mathrm{fm} \approx 3\cdot 10^{-4}\mathrm{eV}eV^{-1}$. We also take into account that the typical value of v_F in Dirac semimetals is of the order of $\sim 1/200$ of the speed of light. In our estimates let us consider the normalized emergent magnetic flux $\frac{\hat\Phi}{2\pi}$ close to the mentioned value 0.85 (so that $F = 1$). Then the typical value of total conductance at the dislocation (127) is

$$\sigma_{zz}^{\mathrm{tot}} \sim 2\cdot\frac{3v_F^3}{4\pi^4T^2D_5} \sim 1\cdot 10^{-2}\mathrm{eV}^{-1}\,. \tag{137}$$

For example, the value of the electric field expressed in the SI system of units, $E = 1\,\mathrm{V/cm}$ corresponds to $E \sim 2\cdot 10^{-5}$ $[\mathrm{eV}]^2$ if expressed in the relativistic units (in our units the electric field strength definition includes the factor e). It produces electric current that is equal (in relativistic units) to $2\cdot 10^{-7}\mathrm{eV} \approx 1\mathrm{m}^{-1}$. In SI this current corresponds to about $0.5\cdot 10^{-10}\mathrm{A} = 0.05\mathrm{nA}$.

Thus we come to the estimate of the order of magnitude of conductance expressed in the usual units

$$\sigma_{zz}^{\mathrm{tot}} \sim 0.05\,\frac{\mathrm{nA}\cdot\mathrm{cm}}{\mathrm{V}} \qquad \text{at}\ \ T \sim 300\,K. \tag{138}$$

for the chose value of the flux, $\Phi = 0.85\,\Phi_0$. In other words, a dislocation carrying the emerging magnetic flux which is about 15% smaller than the elementary flux $\Phi \approx \Phi_0 = 2\pi$, should carry the total electric current $J_z \approx 0.05\,\mathrm{nA}$ due to the electric field of strength $E_z = 1\,\mathrm{V/cm}$ directed along the dislocation axis. If the flux is very close to the critical value, say $\Phi = 0.99\Phi_0$, then the factor F is two order of magnitude larger ($F \approx 134$), and the conductance (138) increases by two orders of magnitude.

Due to strong temperature dependence of the total conductance (127), at small temperature the conductance should increase drastically. For example,

$$\sigma_{zz}^{\mathrm{tot}} \sim 30\,\mathrm{nA\,cm/V}, \qquad \text{at}\ \ T \sim 10\,K, \tag{139}$$

(for reference, here we quote the result for $\Phi = 0.85\Phi_0$ at which $F \approx 1$).

Finally, let us represent the expression for conductance restoring $\hbar$, e and k_B:

$$\sigma_{zz}^{\mathrm{tot}} = n_D\frac{3e^2\hbar v_F^3\,\cos\Theta_{\boldsymbol{En}}}{4\pi^4(k_BT)^2D_5}F\left(|\hat\Phi| - [|\hat\Phi|], \frac{\xi}{L_V}\right), \tag{140}$$

where we have restored the dependence on the conductance on the angle $\Theta_{\boldsymbol{En}}$ between the direction of the external electric field and the dislocation axis [this dependence following directly from the expressions for the chiral anomaly (85) and (86)].

In Eq. (140) the function $F(\alpha, x)$, given by Eq. (128), is represented in Fig. 4. Notice, that the value of $\sigma_{zz}^{\mathrm{tot}}$

depends strongly on $\hat{\Phi}$. For small values of the Burgers vector the value of $\hat{\Phi}$ may be much smaller than unity. Say, in Na_3Bi the minimal topological contribution to $\hat{\Phi}$ is of the order of 0.1 (see Section III). If the contribution of the material-dependent second term to the emergent magnetic flux (38) is neglected, then in this case the value of $\sigma^{\rm tot}$ is suppressed by a small value of the factor $F(\alpha, x)$. However, choosing larger values of the component b_3 of Burgers vector the value of $\hat{\Phi}$ may always be made close to unity, which increases the numerical value of the total conductance by many orders of magnitude. The contribution of the second term to the magnetic flux in Eq. (38) also increases the total value of $\hat{\Phi}$. The conductance should also be increased in a "forest" of dislocations, which are parallel to each other.

Notice that the anomalous contribution to the total conductance originating from the chiral anomaly and the (intrinsic) chiral magnetic effect (140) comes along with the ordinary Ohmic contribution to conductance. The anomalous conductance should depend on the orientation of the electric field with respect to the axis of the dislocation via the angle $\Theta_{\boldsymbol{En}}$ in Eq. (140), and in the case when the dislocation and the electric field are perpendicular to each other, the axial anomaly is no more effective and the anomalous conductance vanishes.

XI. CONCLUSIONS

In this work we discussed intrinsic chiral magnetic effect in Dirac semimetals Na_3Bi and Cd_3As_2 caused by the dislocations. This effect exists without any external magnetic field unlike the conventional chiral magnetic effect that was discussed for Dirac semimetals, for example, in [4]. The dislocation appears as a source of the emergent magnetic field: it carries the emergent magnetic flux. This flux gives rise to the zero mode of the one - particle Hamiltonian localized in the area of size ξ_0 around the dislocation (where $1/\xi_0$ is the infrared cutoff of the field theoretical approximation used in our approach). Length ξ_0 may also be identified with the mean free path of the quasiparticles. For example, for Cd_3As_2 it is of the order of $200\,\mu$m. This zero mode corresponds to the branch of spectrum of the quasiparticles with the spin directed along the magnetic flux of the dislocation.

In the presence of external electric field the spectral flow along this branch of spectrum results in the pumping of the quasiparticles from vacuum. Therefore, the chiral anomaly appears given by Eq. (91). Effective magnetic field entering Eq. (91) differs from the emergent magnetic field of the low energy effective field theory. Instead this field is given by Eq. (92) and is expressed through the wave function of the mentioned zero mode.

This chiral anomaly gives rise to the chiral chemical potential distributed around the dislocation. The characteristic length L_V of this distribution is of the order of $2\,\mu$m for Cd_3As_2. The presence of this chiral chemical potential, in turn, drives the chiral magnetic effect: electric current appears along the dislocation proportional to the field $\boldsymbol{B}$ of Eq. (91). We estimate the corresponding contribution to total conductance. It appears, that this contribution depends strongly on the emergent magnetic flux incident at the dislocation according to Eq. (140). For the values of magnetic flux close to 2π the estimated value of the contribution to conductance is of the order of $0.05\,\mathrm{nA\,cm/V}$ for $T \approx 300\,K$ and of the order of $30\,\mathrm{nA\,cm/V}$ for $T \approx 10\,K$. Notice, that multiple dislocations multiply the CME contribution to the total conductance of Dirac semimetal. Several dislocations with Burgers vectors $\boldsymbol{b}_i$ and distances between them mush smaller, than L_V, work effectively as a single dislocation with the Burgers vector $\sum_i \boldsymbol{b}_i$. In principle, the crystal growth may be organised in such a way, that the dislocations appear along the chosen direction with the chosen values of the Burgers vector. Also the dislocations appear as a result of plastic deformations of the crystals. This opens the possibility to observe chiral magnetic effect experimentally.

ACKNOWLEDGMENTS

The work of M.A.Z. was supported by Ministry of science and education of Russian Federation under the contract 02.A03.21.0003 and by grant RFBR 14-02-01261. The work of M.N.C. and M.A.Z. was partially supported by Far Eastern Federal University grant 13-09-0617-m_a. M.A.Z. is grateful to the members of Laboratoire de Mathématiques et Physique Théorique (Tours, France) for the kind hospitality extended to him during his stay.

[1] Z. K. Liu et al., *"Discovery of a Three-dimensional Topological Dirac Semimetal, Na_3Bi"*, Science (2014) **343**, 864 [arXiv:1310.0391].

[2] M. Neupane et al., "Observation of a topological 3D Dirac semimetal phase in high-mobility Cd_3As_2" Nature Commun. **05**, 3786 (2014) [arXiv:1309.7892].

[3] S. Borisenko et al., "Experimental Realization of a Three-Dimensional Dirac Semimetal", Phys. Rev. Lett. **113**, 027603 (2014) [arXiv:1309.7978].

[4] Q. Li et al., arXiv:1412.6543; R. Y. Chen et al., *"Optical spectroscopy study of three dimensional Dirac semimetal $ZrTe_5$"*, arXiv:1505.00307

[5] Devendra Kumar, Archana Lakhani, *"Observation of three-dimensional Dirac semimetal state in topological insulator Bi_2Se_3"*, arXiv:1504.08328.

[6] Cheng Zhang et al, *"Detection of chiral anomaly and valley transport in Dirac semimetals"*, arXiv:1504.07698.

[7] Tian Liang et al, *Ultrahigh mobility and giant magnetoresistance in the Dirac semimetal Cd_3As_2*, Nature Mater. **14**, 280 (2015) [arXiv:1404.7794].

[8] Hemian Yi et al., *Evidence of Topological Surface State in Three-Dimensional Dirac Semimetal Cd_3As_2*, Sci. Rep. **4**, 6106 (2014) [arXiv:1405.5702].

[9] Z. K. Liu et al., *A stable three-dimensional topological Dirac semimetal Cd_3As_2*, Nature Mater. **13**, 677 (2014).

[10] L. P. He et al., *Quantum Transport Evidence for the Three-Dimensional Dirac Semimetal Phase in Cd_3As_2*, Phys. Rev. Lett. **113**, 246402 (2014) [arXiv:1404.2557].

[11] B. Q. Lv et al., *"Experimental discovery of Weyl semimetal TaAs"*, arXiv:1502.04684; X. Huang, *"Observation of the chiral anomaly induced negative magneto-resistance in 3D Weyl semi-metal TaAs"*, arXiv:1503.01304; B. Q. Lv et al., *"Observation of Weyl nodes in TaAs"* arXiv:1503.09188.

[12] X. Wan, A. M. Turner, A. Vishwanath, and S. Y. Savrasov, *"Topological semimetal and fermi-arc surface states in the electronic structure of pyrochlore iridates"*, Phys. Rev. B **83**, 205101 (2011) [arXiv:1007.0016].

[13] A. M. Turner, A. Vishwanath, and C. O. Head, *"Beyond band insulators: Topology of semi-metals and interacting phases"*, Topological Insulators 6 (2013) 293 [arXiv:1301.0330].

[14] G. B. Halsasz and L. Balents, *"Time-reversal invariant realization of the Weyl semimetal phase"*, Phys. Rev. B **85**, 035103 (2012).

[15] F. Haldane, *"Attachment of surface "fermi arcs" to the bulk fermi surface: fermi-level plumbing" in topological metals"*, arXiv:1401.0529 .

[16] S. Matsuura, P.-Y. Chang, A. P. Schnyder, and S. Ryu, *"Protected boundary states in gapless topological phases"*, New Journal of Physics **15**, 065001 (2013).

[17] S. Parameswaran, T. Grover, D. Abanin, D. Pesin, and A. Vishwanath, *"Probing the chiral anomaly with nonlocal transport in Weyl semimetals*, Phys. Rev. X **4**, 031035 (2014) [arXiv:1306.1234].

[18] M. N. Chernodub, A. Cortijo, A. G. Grushin, K. Landsteiner, and M. A. Vozmediano, *"A condensed matter realization of the axial magnetic effect"*, Phys. Rev. B **89**, 081407(R) (2014) [arXiv:1311.0878].

[19] Z. Jian-Hui, J. Hua, N. Qian, and S. Jun-Ren, *"Topological invariants of metals and the related physical effects"*, Chinese Phys. Lett. **30**, 027101 (2013) [arXiv:1211.0772].

[20] P. Hosur, *"Friedel oscillations due to Fermi arcs in Weyl semimetals"*, Phys. Rev. B **86**, 195102 (2012) [arXiv:1208.0027].

[21] M. Vazifeh and M. Franz, *"Electromagnetic response of weyl semimetals"*, Phys. Rev. Lett. **111**, 027201 (2013) [arXiv:1303.5784].

[22] Y. Chen, S. Wu, and A. Burkov, *"Axion response in Weyl semimetals"*, Phys. Rev. B **88**, 125105 (2013) [arXiv:1306.5344].

[23] Y. Chen, D. Bergman, and A. Burkov, *"Weyl fermions and the anomalous Hall effect in metallic ferromagnets"*, Phys. Rev. B **88**, 125110 (2013) [arXiv:1305.0183]; David Vanderbilt, Ivo Souza, and F. D. M. Haldane Phys. Rev. B **89**, 117101 (2014) [arXiv:1312.4200].

[24] S. T. Ramamurthy and T. L. Hughes, *"Patterns of electro-magnetic response in topological semi-metals"*, arXiv:1405.7377.

[25] K. Fukushima, D. E. Kharzeev and H. J. Warringa, Phys. Rev. D **78**, 074033 (2008) [arXiv:0808.3382].

[26] Hui Li et al., *"Negative Magnetoresistance in Dirac Semimetal Cd_3As_2"*, arXiv:1507.06470; Cheng Zhang et al., *"Detection of chiral anomaly and valley transport in Dirac semimetals"*, arXiv:1504.07698; Cai-Zhen Li et al., *"Giant negative magnetoresistance induced by the chiral anomaly in individual Cd_3As_2 nanowires"*, arXiv:1504.07398; Jun Xiong et al., *"Signature of the chiral anomaly in a Dirac semimetal: a current plume steered by a magnetic field"*, arXiv:1503.08179; Jan Behrends, Adolfo G. Grushin, Teemu Ojanen, Jens H. Bardarson, *"Visualizing the chiral anomaly in Dirac and Weyl semimetals with photoemission spectroscopy"*, arXiv:1503.04329; Chenglong Zhang et al., *"Observation of the Adler-Bell-Jackiw chiral anomaly in a Weyl semimetal"*, arXiv:1503.02630; Jun Xiong, Satya Kushwaha, Jason Krizan, Tian Liang, R. J. Cava, N. P. Ong, *"Anomalous conductivity tensor in the Dirac semimetal Na_3Bi"*, arXiv:1502.06266.

[27] Fernando de Juan, Juan L. Mañes, María A. H. Vozmediano, *"Gauge fields from strain in graphene"*, Phys. Rev. B **87**, 165131 (2013) [arXiv:1212.0924].

[28] Fernando de Juan, Mauricio Sturla, Maria A. H. Vozmediano, *"Space dependent Fermi velocity in strained graphene"*, Phys. Rev. Lett. 108, 227205 (2012) [arXiv:1201.2656].

[29] M. A. H. Vozmediano, M. I. Katsnelson, F. Guinea, *"Gauge fields in graphene"*, Phys. Rep. **496**, 109 (2010) [arXiv:1003.5179].

[30] Alberto Cortijo, Francisco Guinea, María A. H. Vozmediano, *"Geometrical and topological aspects of graphene and related materials"*, J. Phys. A: Math. Theor. **45**, 383001 (2012) [arXiv:1112.2054].

[31] Juan L. Mañes, Fernando de Juan, Mauricio Sturla, Maria A. H. Vozmediano, *"Generalized effective Hamiltonian for graphene under nonuniform strain"*, Phys. Rev. **88**, 155405 (2013) [arXiv:1308.1595].

[32] G.E. Volovik and M.A. Zubkov, *"Emergent gravity in graphene"*, talk presented at the International Moscow Phenomenology Workshop (July 21-25, 2013), arXiv:1308.2249.

[33] G.E. Volovik and M.A. Zubkov, *"Emergent Hořava gravity in graphene"*, Ann. Phys. **340**, 352 (2014) [arXiv:1305.4665].

[34] G. E. Volovik and M. A. Zubkov, *"Emergent geometry experienced by fermions in graphene in the presence of dislocations,"* Annals Phys. **356** 255 (2015) [arXiv:1412.2683].

[35] Alberto Cortijo, Yago Ferreirós, Karl Landsteiner, María A. H. Vozmediano, *"Hall viscosity from elastic gauge fields in Dirac crystals"*, arXiv:1506.05136.

[36] G.E. Volovik, *"The Universe in a Helium Droplet"*, Clarendon Press, Oxford (2003)

[37] Onkar Parrikar, Taylor L. Hughes, and Robert G. Leigh, *"Torsion, parity-odd response, and anomalies in topological states"*, Phys. Rev. D **90**, 105004 (2014) [arXiv:1407.7043].

[38] M.A.Zubkov, *"Emergent gravity and chiral anomaly in Dirac semimetals in the presence of dislocations"*, Annals of Phys., **360**, 655 (2015), [arXiv:1501.04998]

[39] L.D. Landau, E.M. Lifshitz, *"Theory of Elasticity, Third Edition: Volume 7 (Course of Theoretical Physics)"*, Butterworth-Heinemann, Oxford (1986).

[40] G. E. Volovik, M. A. Zubkov, *"Emergent Weyl spinors in multi-fermion systems"*, Nucl. Phys. B **881**, 514 (2014)

[arXiv:1402.5700].

[41] Satya K. Kushwaha et al., *"Bulk crystal growth and electronic characterization of the 3D Dirac Semimetal Na_3Bi"*, APL Mater. **3**, 041504 (2015) [arXiv:1502.03547].

[42] M.M. Ansourian, *"Index theory and the axial current anomaly in two dimensions"*, Phys. Lett. B **70**, 301 (1977).

[43] Problems to Section 27 of Ref. [39]; see also a derivation in Ref. [38].

[44] Ying Ran, Yi Zhang and Ashvin Vishwanath, *"One-dimensional topologically protected modes in topological insulators with lattice dislocations"*, Nature Phys. **5**, 298 (2009).

[45] Zhijun Wang, Yan Sun, Xingqiu Chen, Cesare Franchini, Gang Xu, Hongming Weng, Xi Dai, Zhong Fang, *"Dirac semimetal and topological phase transitions in A_3Bi (A=Na, K, Rb)"*, Phys. Rev. B **85**, 195320 (2012) [arXiv:1202.5636].